Z. Angew. Math. Phys. 66 (2015), 3447–3471

0044-2275/15/063447-25
published online July 15, 2015
DOI 10.1007/s00033-015-0555-5

Zeitschrift für angewandte Mathematik und Physik ZAMP

Stability of axisymmetric liquid bridges

Leonid G. Fel and Boris Y. Rubinstein

Abstract. Based on the Weierstrass representation of second variation, we develop a non-spectral theory of stability for isoperimetric problem with minimized and constrained two-dimensional functionals of general type and free endpoints allowed to move along two given planar curves. We establish the stability criterion and apply this theory to the axisymmetric liquid bridge between two axisymmetric solid bodies without gravity to determine the stability of menisci with free contact lines. For catenoid and cylinder menisci and different solid shapes, we determine the stability domain. The other menisci (unduloid, nodoid and sphere) are considered in a simple setup between two plates. We find the existence conditions of stable unduloid menisci with and without inflection points.

Mathematics Subject Classification. Primary 53A10 · Secondary 76B45.

Keywords. Capillarity · Liquid bridge · Stability criteria · Jacobi equation.

1. Introduction

A capillary surface is an interface separating two non-mixing fluids adjacent to each other. Its shape depends on liquid volume and on boundary conditions (BC) specified at the contact line (CL) where the liquids touch the solid. A liqud bridge (LB) is one of the well studied among different types of drops (sessile, pendant [28], etc.). It emerges when a small amount of fluid forms an axisymmetric LB with interface (*meniscus*) between two axisymmetric solids. A history of the LB problem in the absence of gravity shows a remarkable interaction between theoretical physics and pure mathematics and can be traced in two directions: evolution of menisci shapes (including their volume V, surface area S and surface curvature H) and study of their stability.

Delaunay [5] was the first who classified all surfaces of revolution with constant mean curvature (CMC) in his study of the Young–Laplace equation (YLE). These are cylinder (Cyl), sphere (Sph), catenoid (Cat), nodoid (Nod) and unduloid (Und). Later Beer [2] gave analytical solutions of YLE in elliptic integrals, and Plateau [17] supported the theory by experimental observations. For a whole century, almost no rigorous results were reported on the computation of H, V and S of LB. In the 1970s, Orr et al. [16] gave such formulas for all menisci types in case of a solid sphere contacting a solid plate. A new insight into the problem was presented recently in [19] for the case of separated solid sphere and plate as a nonlinear eigenvalue equation with a discrete spectrum of menisci and their curvature. The existence of multiple solutions of YLE for given LB volume reported in [19] poses a question of local stability of menisci.

The first step toward the modern theory of LB stability was made by Sturm [22] in appendix to [5], characterizing CMC surfaces as the solutions to isoperimetric problem (**IP**). Such relationship between a second-order differential equation and a functional E reaching its extremal value was known at the time. The main tool for this problem is a calculus of variations whose basis was laid in the 1870s by Weierstrass in his unpublished lectures [27] and extended by Bolza [3] and others. The difficult part of the theory deals with the second variation $\delta^2 E$ in vicinity of solutions of the Euler–Lagrange equations (ELE) where a perturbation w acts.

The **IP** with *fixed endpoints* t_1, t_2 was studied first by Weierstrass who derived a determinant equation [27], p. 275, which defines an existence of conjugate points. Later Howe [11] applied Weierstrass' theory to study the LB problem with *fixed CL*. This approach continued to be used in different setups (see, e.g., [6,9]). Another type of variational **IP** with *free endpoints* allowed to move along two given planar curves S_1, S_2 is important for stability of axisymmetric LB with *free CL*. An expression for $\delta^2 E$ for **IP** with fixed endpoints was derived by Weierstrass, while a similar expression for **IP** with free endpoints is still awaiting its derivation (see [8] for a comprehensive introduction).

The **IP** providing $\Xi_0[w] = \min$ with an integrand quadratic in w, w', linear constraint $\Xi_1[w] = 0$ and *fixed* BC $w(t_j) = 0$ is related to an eigenvalue problem associated with a linear operator (see [4], Chap. 6). This is true even if the fixed BC is replaced by any other linear homogeneous BC (Dirichlet, Neumann or mixed) and also is consistent with normalization $\Xi_2[w] = \int_{t_2}^{t_1} w^2 \mathrm{d}t = 1$. Thus, the **IP** for the functional $\Xi_0[w] + \mu\Xi_1[w] - \lambda\Xi_2[w]$ with two Lagrange multipliers μ, λ and constraints Ξ_1, Ξ_2 leads to the Sturm–Liouville equation (SLE) with real spectrum $\{\lambda_n\}$ and stability criterion: $\min\{\lambda_n\} > 0$. A study of the SLE spectrum is a complicated task for generic curves S_1, S_2. Such approach was implemented [15] to study the stability of LB with fixed CL.

In the 1980s, Th. Vogel suggested another approach to the LB problem with *free CL* constructing an associated SLE with Neumann BC instead of Dirichlet BC and established the stability criterion valid for LB between plates [23,24]. This method requires to solve the eigenvalue problem and to consider the behavior of the two first minimal eigenvalues λ_1, λ_2. Implementation of this step is a difficult task in the case of Und and Nod menisci. That is why only some exact results for Cat [29], Sph [21] and Und [7] menisci between two plates are known. Study of LB stability between other surfaces encounters even more difficulties. This was done only for Cyl [25] and (qualitatively) for convex Und and Nod [26] between equal solid spheres. This method [26] allows to consider also a stability with respect to asymmetric perturbations. No results on stability of menisci between other solids (similar or different) are reported. There exists another class of problems dealing with stability of LB inside containers [18,20].

Based on the Weierstrass representation of second variation, we develop a non-spectral theory of stability for **IP** with the minimized $E[x, y]$ and constrained $V[x, y]$ functionals of general type and with free endpoints belonging to generic curves. We derive the expression for $\delta^2 E$ and find when it is positive definite; we apply this theory to Delaunay surfaces and axisymmetric solid bodies to determine the stability of meniscus with free CL under axisymmetric perturbations.

In Sects. 2, 3 and 4, we recall a setup of **IP** with fixed endpoints and Weierstrass' formula for $\delta^2 E$ with stability criterion based on which we derive *the stability criterion for free endpoints* in closed form (Theorem 4.1). In Sect. 2, we derive two ELE supplemented with transversality BC and find its extremal solution $\bar{x}(t), \bar{y}(t)$ which serves as a functional parameter in formulation of **IP** for the second variation $\Xi_0[w] = \delta^2 E[x, y]$ with constraint $\Xi_1[w] = \delta V[x, y] = 0$. In Sect. 3, this leads to the Jacobi equation with homogeneous BC $w(t_j) = 0$ for perturbation $w(t)$. Its solutions produce the necessary condition of stability (the criterion of conjugate points absence) that generate the stability domain $\mathsf{Stab}_1(t_2, t_1)$ for extremal solution in the $\{t_1, t_2\}$-plane. In Sect. 4 we derive the expression for $\delta^2 E[x, y]$ as a quadratic form in small perturbations $\delta\tau_j$ of the meniscus free endpoints along the curves $S_j(\tau_j)$ and find a domain $\mathbb{Q}(t_2, t_1)$ where $\delta^2 E[x, y]$ is positive definite. Finally, we find the stability domain $\mathsf{Stab}_2(t_2, t_1)$ for extremal solution with free endpoints as intersection of Stab_1 and $\mathbb{Q}$ that exhibits a new method to analyze the stability of LB between solid bodies under axisymmetric perturbations.

In Sects. 5 and 6, this approach is applied to study the stability of axisymmetric LB between solid bodies in absence of gravity. For Cat and Cyl menisci, we consider different solid shapes and calculate Stab_2. Among new results, we verify the solutions for Cat menisci between two plates [29] and Cyl menisci between two spheres [25] obtained in the framework of Vogel's theory. The other menisci are treated in Sect. 6.2 in a simple setup between two plates. We find the existence conditions of stable Und menisci with and without inflection point and verify conclusions formulated in [1,7,23,24] on their stability for special contact angles. The coincidence of stability conditions of axisymmetric LB under generic (axisymmetric

and asymmetric) disturbances considered in [1,7,23–25,29] and under only axisymmetric disturbances presented in this work shows that the latter are the most dangerous of generic disturbances destroying these LBs. Stability of Und, Nod and Sph menisci between non-planar bodies will be considered in the separate paper.

2. Stability as an isoperimetric problem with free endpoints

Let a planar curve C with parametrization $\{x(t), y(t)\}$, $t_2 \le t \le t_1$, be given with its endpoints $\{x(t_j), y(t_j)\}$, $j = 1, 2$ allowed to move (see Fig. 1) along two given curves S_j parametrized as $\{X_j(\tau_j), Y_j(\tau_j)\}$, $0 \le \tau_j \le \tau_j^*$ (variable τ_j runs along S_j).

Consider the first isoperimetric problem (**IP-1**) for the functional $E[x, y]$,

$$E[x,y] = \int_{t_2}^{t_1} \mathsf{E}(x, y, x_t, y_t)\mathrm{d}t + \sum_{j=1}^{2} \int_0^{\tau_j^*} \mathsf{A}_j(X_j, Y_j, X_{j,\tau_j}, Y_{j,\tau_j})\mathrm{d}\tau_j, \tag{2.1}$$

with constraint $V[x, y] = 1$ imposed on functional,

$$V[x,y] = \int_{t_2}^{t_1} \mathsf{V}(x, y, x_t, y_t)\mathrm{d}t + \sum_{j=1}^{2} (-1)^j \int_0^{\tau_j^*} \mathsf{B}_j(X_j, Y_j, X_{j,\tau_j}, Y_{j,\tau_j})\mathrm{d}\tau_j, \tag{2.2}$$

where we denote $f_t = f' = \mathrm{d}f/\mathrm{d}t$ and $F_{k,t} = F_k' = \mathrm{d}F_k/\mathrm{d}t$.

The integrands E and V should be positive homogeneous functions of degree one in x_t and y_t, e.g., $\mathsf{E}(x, y, kx_t, ky_t) = k\mathsf{E}(x, y, x_t, y_t)$, that results in identities stemming from Euler theorem for homogeneous functions,

$$\mathsf{E} = \frac{\partial \mathsf{E}}{\partial x'} x_t + \frac{\partial \mathsf{E}}{\partial y'} y_t, \quad \mathsf{A}_j = \frac{\partial \mathsf{A}_j}{\partial X_{j,\tau_j}} X_{j,\tau_j} + \frac{\partial \mathsf{A}_j}{\partial Y_{j,\tau_j}} Y_{j,\tau_j}, \tag{2.3}$$

and similar relations for V and B_j.

We have to find an extremal curve $\bar{C} = \{\bar{x}(t), \bar{y}(t)\}$ with free endpoints $\bar{x}(t_j), \bar{y}(t_j)$ which belong to two given curves S_j such that the functional $E[x, y]$ reaches its minimum, while the other functional $V[x, y]$ is constrained.

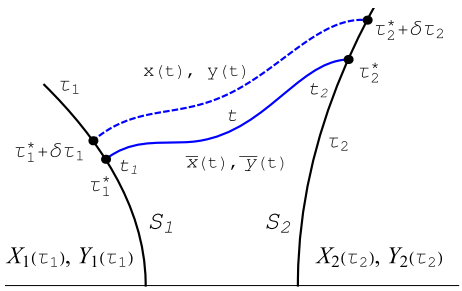

FIG. 1. A sketch of variation of extremal curve $\{\bar{x}(t), \bar{y}(t)\}$ with free endpoints $\bar{x}(t_j), \bar{y}(t_j)$, $j = 1, 2$, which belong to the two given curves S_1, S_2 such that the functional $E[x, y]$ reaches its minimum while $V[x, y]$ is constrained. Extremal (*solid*) and disturbed (*dashed*) curves are drawn in *blue*

Define a functional $W[x,y] = E[x,y] - \lambda V[x,y]$ with the multiplier λ

$$W[x,y] = \int_{t_2}^{t_1} F(x,y,x_t,y_t)\mathrm{d}t - \sum_{j=1}^{2}(-1)^j \int_0^{\tau_j^*} G_j(X_j, Y_j, X_{j,\tau_j}, Y_{j,\tau_j})\mathrm{d}\tau_j, \tag{2.4}$$

where $F = \mathsf{E} - \lambda\mathsf{V}$, $G_1 = \lambda\mathsf{B}_1 + \mathsf{A}_1$, $G_2 = \lambda\mathsf{B}_2 - \mathsf{A}_2$. According to (2.3) we have

$$F = \frac{\partial F}{\partial x_t}x_t + \frac{\partial F}{\partial y_t}y_t, \quad G_j = \frac{\partial G_j}{\partial X_{j,\tau_j}}X_{j,\tau_j} + \frac{\partial G_j}{\partial Y_{j,\tau_j}}Y_{j,\tau_j}. \tag{2.5}$$

Calculate the total variation of the functional, $\mathbb{D}W = \mathbb{D}_0 W + \mathbb{D}_1 W - \mathbb{D}_2 W$,

$$\begin{aligned} \mathbb{D}_0 W &= \int_{t_2}^{t_1} [F + \Delta_1 F + \Delta_2 F + \cdots]\,\mathrm{d}t - \int_{t_2}^{t_1} F\mathrm{d}t, \\ \mathbb{D}_j W &= \int_0^{\tau_j^*+\delta\tau_j} G_j \mathrm{d}\tau_j - \int_0^{\tau_j^*} G_j \mathrm{d}\tau_j, \end{aligned} \tag{2.6}$$

where

$$\begin{aligned} \Delta_1 F &= \frac{\partial F}{\partial x}u + \frac{\partial F}{\partial x_t}u' + \frac{\partial F}{\partial y}v + \frac{\partial F}{\partial y_t}v', \\ \Delta_2 F &= \frac{u^2}{2}\frac{\partial^2 F}{\partial x^2} + uu'\frac{\partial^2 F}{\partial x \partial x_t} + \frac{u'^2}{2}\frac{\partial^2 F}{\partial x_t^2} + \frac{v^2}{2}\frac{\partial^2 F}{\partial y^2} + vv'\frac{\partial^2 F}{\partial y \partial y_t} \\ &\quad + \frac{v'^2}{2}\frac{\partial^2 F}{\partial y_t^2} + uv\frac{\partial^2 F}{\partial x \partial y} + uv'\frac{\partial^2 F}{\partial x \partial y_t} + u'v\frac{\partial^2 F}{\partial x_t \partial y} + u'v'\frac{\partial^2 F}{\partial x_t \partial y_t}, \end{aligned} \tag{2.7}$$

and $\{u(t), v(t)\}$ is a small perturbation in vicinity of curve $\bar{C}$ where the extremum of **IP-1** is reached. Define a projection of the $\{u(t), v(t)\}$ vector on the normal to $\{\bar{x}(t), \bar{y}(t)\}$,

$$\widetilde{w}(t) = u\,\bar{y}_t - v\,\bar{x}_t. \tag{2.8}$$

Represent $\mathbb{D}_0 W$ and $\mathbb{D}_j W$ up to the terms quadratic in $\delta\tau_j, u, v, u', v'$,

$$\begin{aligned} \mathbb{D}_0 W &= \int_{t_2}^{t_1} \Delta_1 F\mathrm{d}t + \int_{t_2}^{t_1} \Delta_2 F\mathrm{d}t, \quad \mathbb{D}_j W = G_j^*\delta\tau_j + \frac{1}{2}\frac{\mathrm{d}G_j^*}{\mathrm{d}\tau_j}(\delta\tau_j)^2, \\ \frac{\mathrm{d}G_j^*}{\mathrm{d}\tau_j} &= \frac{\partial G_j^*}{\partial X_j}\frac{\mathrm{d}X_j}{\mathrm{d}\tau_j} + \frac{\partial G_j^*}{\partial Y_j}\frac{\mathrm{d}Y_j}{\mathrm{d}\tau_j} + \frac{\partial G_j^*}{\partial X_j'}\frac{\mathrm{d}^2 X_j}{\mathrm{d}\tau_j^2} + \frac{\partial G_j^*}{\partial Y_j'}\frac{\mathrm{d}^2 Y_j}{\mathrm{d}\tau_j^2}, \end{aligned} \tag{2.9}$$

where $G_j^* = G_j$ and $\partial G_j^*/\partial X_j = \partial G_j/\partial X_j$ computed at $\tau_j = \tau_j^*$.

2.1. First variation δW and Euler–Lagrange equations

Using the terms in (2.9) linear in $\delta\tau_j$, u, v and u_t, v_t, in (2.6) calculate δW

$$\delta W = \int_{t_2}^{t_1} \Delta_1 F\mathrm{d}t + G_1^*\delta\tau_1 - G_2^*\delta\tau_2. \tag{2.10}$$

To derive BC for perturbations $u(t_j), v(t_j)$, we have to make them consistent with free endpoints running along the curves S_j

$$\begin{aligned} \bar{x}(t_j) &= X(\tau_j^*), \quad \bar{x}(t_j) + u(t_j) = X(\tau_j^* + \delta\tau_j), \\ \bar{y}(t_j) &= Y(\tau_j^*), \quad \bar{y}(t_j) + v(t_j) = Y(\tau_j^* + \delta\tau_j), \end{aligned} \tag{2.11}$$

resulting in a sequence of equalities: $u(t_j) = \sum_{k=1}^{\infty} u_k(t_j)$ and $v(t_j) = \sum_{k=1}^{\infty} v_k(t_j)$,

$$u_k(t_j) = \frac{1}{k!}\frac{\mathrm{d}^k X_j}{\mathrm{d}\tau_j^k}(\delta\tau_j)^k, \quad v_k(t_j) = \frac{1}{k!}\frac{\mathrm{d}^k Y_j}{\mathrm{d}\tau_j^k}(\delta\tau_j)^k. \tag{2.12}$$

A function $w(t) = u_1\bar{y}_t - v_1\bar{x}_t$ is a linear in $\delta\tau_j$ part of $\widetilde{w}(t)$ in (2.8); it reads at the endpoints,

$$w(t_j) = \eta(t_j, \tau_j^*)\delta\tau_j, \quad \eta(t_j, \tau_j^*) = \bar{y}_t\frac{\mathrm{d}X_j}{\mathrm{d}\tau_j} - \bar{x}_t\frac{\mathrm{d}Y_j}{\mathrm{d}\tau_j}. \tag{2.13}$$

Denote by $\delta F/\delta z = \partial F/\partial z - \frac{\mathrm{d}}{\mathrm{d}t}(\partial F/\partial z')$ the variational derivative. Then δW in (2.10) may be written as

$$\delta W = \int_{t_2}^{t_1}\left(u\frac{\delta F}{\delta x} + v\frac{\delta F}{\delta y}\right)\mathrm{d}t + \left[u_1\frac{\partial F}{\partial x'} + v_1\frac{\partial F}{\partial y'}\right]_{t_2}^{t_1} + G_1^*\delta\tau_1 - G_2^*\delta\tau_2.$$

Substitute $u_1(t_j)$ and $v_1(t_j)$ from (2.12) into the last expression and obtian

$$\delta W = \int_{t_2}^{t_1}\left(u\frac{\delta F}{\delta x} + v\frac{\delta F}{\delta y}\right)\mathrm{d}t - \sum_{j=1}^{2}(-1)^j\left[\frac{\partial F_j}{\partial x'}\frac{dX_j}{d\tau_j} + \frac{\partial F_j}{\partial y'}\frac{dY_j}{d\tau_j} + G_j^*\right]\delta\tau_j,$$

where $F_j = F$, $\partial F_j/\partial x = \partial F/\partial x$, etc. computed at $t = t_j$. Thus, we get ELE

$$\frac{\partial F}{\partial x} - \frac{\mathrm{d}}{\mathrm{d}t}\frac{\partial F}{\partial x'} = 0, \quad \frac{\partial F}{\partial y} - \frac{\mathrm{d}}{\mathrm{d}t}\frac{\partial F}{\partial y'} = 0, \tag{2.14}$$

supplemented by the transversality conditions:

$$\frac{\partial F_2}{\partial x'}\frac{dX_2}{d\tau_2} + \frac{\partial F_2}{\partial y'}\frac{dY_2}{d\tau_2} + G_2^* = 0, \quad \frac{\partial F_1}{\partial x'}\frac{dX_1}{d\tau_1} + \frac{\partial F_1}{\partial y'}\frac{dY_1}{d\tau_1} + G_1^* = 0. \tag{2.15}$$

Solution $\bar{x}(t), \bar{y}(t)$ gives the extremal value of $E[x, y]$ and constraint $V[x, y] = 1$.

Identify $E[x, y]$ as a functional of surface energy of LB and fix its volume by variational constraint $V[x, y] = 1$. Then we arrive at the LB problem [19] in absence of gravity where ELE (2.14) and transversality conditions (2.15) are known as YLE and Young relations. The latter leaves free the values $x(t_j)$, $y(t_j)$ at the endpoints where the meniscus contacts the solid surfaces at the fixed contact angles.

2.2. The Weierstrass representation of second variation $\delta^2 W$

Making use in (2.6) of the terms quadratic in $\delta\tau_j$, u_1, v_1 u_1', v_1', and linear in u_2, v_2 calculate the second variation,

$$\delta^2 W = \int_{t_2}^{t_1}\Delta_2 F\mathrm{d}t + \left(\frac{\partial F}{\partial x'}u_2 + \frac{\partial F}{\partial y'}v_2\right)_{t_2}^{t_1} + \frac{1}{2}\left(\frac{\mathrm{d}G_1}{\mathrm{d}\tau_1}(\delta\tau_1)^2 - \frac{\mathrm{d}G_2}{\mathrm{d}\tau_2}(\delta\tau_2)^2\right) \tag{2.16}$$

Substituting u_2 and v_2 from (2.12) into the last expression, we obtain

$$\delta^2 W = \int_{t_2}^{t_1}\Delta_2 F\mathrm{d}t - \frac{1}{2}\sum_{j=1}^{2}(-1)^j\left(\frac{\partial F}{\partial x'}\frac{\mathrm{d}^2 X_j}{\mathrm{d}\tau_j^2} + \frac{\partial F}{\partial y'}\frac{\mathrm{d}^2 Y_j}{\mathrm{d}\tau_j^2} + \frac{\mathrm{d}G_j}{\mathrm{d}\tau_j}\right)(\delta\tau_j)^2.$$

Denote $\delta^2_B W = \int_{t_2}^{t_1} \Delta_2 F \mathrm{d}t$ and following Weierstrass [27], pp. 132–134 (see also Bolza [3], p. 206) represent $\delta^2_B W$ in terms of small perturbation $\{u(t), v(t)\}$ of the extremal curve $\{\bar{x}(t), \bar{y}(t)\}$ and $w(t)$,

$$\delta^2_B W[x,y] = \frac{1}{2}\Xi_0[w] + \frac{1}{2}\left(Lu_1^2 + 2Mu_1v_1 + Nv_1^2\right)|_{t_2}^{t_1}, \tag{2.17}$$

$$\Xi_0[w] = \int_{t_2}^{t_1} \left(H_1 w'^2 + H_2 w^2\right) \mathrm{d}t, \quad M = \begin{cases} F_{xy'} + \bar{x}_t \bar{y}_{tt} H_1, \\ F_{yx'} + \bar{y}_t \bar{x}_{tt} H_1, \end{cases}$$

$$L = F_{xx'} - \bar{y}_t \bar{y}_{tt} H_1, \quad N = F_{yy'} - \bar{x}_t \bar{x}_{tt} H_1, \quad H_1 = \frac{F_{x'x'}}{\bar{y}_t^2} = \frac{F_{y'y'}}{\bar{x}_t^2} = -\frac{F_{x'y'}}{\bar{x}_t \bar{y}_t}, \tag{2.18}$$

$$H_2 = \frac{F_{xx} - \bar{y}_{tt}^2 H_1 - L_t}{\bar{y}_t^2} = \frac{F_{yy} - \bar{x}_{tt}^2 H_1 - N_t}{\bar{x}_t^2} = -\frac{F_{xy} + \bar{x}_{tt}\bar{y}_{tt} H_1 - M_t}{\bar{x}_t \bar{y}_t}.$$

Substituting (2.12) and (2.9) into (2.16), we obtain,

$$\delta^2 W = \delta^2_B W + \xi_1 (\delta\tau_1)^2 - \xi_2 (\delta\tau_2)^2, \tag{2.19}$$

where

$$2\xi_j = \frac{\partial F_j}{\partial x'} \frac{\mathrm{d}^2 X_j}{\mathrm{d}\tau_j^2} + \frac{\partial F_j}{\partial y'} \frac{\mathrm{d}^2 Y_j}{\mathrm{d}\tau_j^2} + \frac{\partial G_j}{\partial X_j} \frac{\mathrm{d}X_j}{\mathrm{d}\tau_j} + \frac{\partial G_j}{\partial Y_j} \frac{\mathrm{d}Y_j}{\mathrm{d}\tau_j} + \frac{\partial G_j}{\partial X_j'} \frac{\mathrm{d}^2 X_j}{\mathrm{d}\tau_j^2} + \frac{\partial G_j}{\partial Y_j'} \frac{\mathrm{d}^2 Y_j}{\mathrm{d}\tau_j^2}.$$

Substitute $u_1(t_j), v_1(t_j)$ from (2.12) into (2.17) and combine it with (2.19),

$$\delta^2 W = \frac{1}{2}\Xi_0[w] + K_1 (\delta\tau_1)^2 - K_2 (\delta\tau_2)^2, \tag{2.20}$$

$$2K_j = 2\xi_j + L(t_j) \left(\frac{\mathrm{d}X_j}{\mathrm{d}\tau_j}\right)^2 + 2M(t_j) \frac{\mathrm{d}X_j}{\mathrm{d}\tau_j} \frac{\mathrm{d}Y_j}{\mathrm{d}\tau_j} + N(t_j) \left(\frac{\mathrm{d}Y_j}{d\tau_j}\right)^2. \tag{2.21}$$

3. Homogeneous boundary conditions: fixed endpoints

Study the stability of the extremal curve $\{\bar{x}(t), \bar{y}(t)\}$ w.r.t. small fluctuations in two different cases considered separately; the first case corresponds to the perturbation of the extremal curve in the interval (t_2, t_1) for the fixed endpoints,

$$u(t_j) = v(t_j) = w(t_j) = 0, \quad j = 1, 2. \tag{3.1}$$

The second case is when at least one endpoint is free and allowed to run along given curves S_j and is discussed in Sect. 4. Start with the second isoperimetric problem (**IP-2**) associated with perturbations $\{u(t), v(t)\}$ in the vicinity of $\{\bar{x}(t), \bar{y}(t)\}$ with BC (3.1). Following Bolza [3], p.215, write the constraint $\delta V[x,y] = 0$,

$$\Xi_1[w] = \int_{t_2}^{t_1} H_3 w \mathrm{d}t = 0, \quad \begin{cases} H_3 = \mathsf{V}_{xy'} - \mathsf{V}_{x'y} + H_4(\bar{x}_t \bar{y}_{tt} - \bar{y}_t \bar{x}_{tt}), \\ H_4 = \mathsf{V}_{x'x'} \bar{y}_t^{-2} = \mathsf{V}_{y'y'} \bar{x}_t^{-2} = -\mathsf{V}_{x'y'} \bar{x}_t^{-1} \bar{y}_t^{-1}, \end{cases} \tag{3.2}$$

which involves perturbation w. For LB problem, we have $\mathsf{V} = x^2 y'$, $\mathsf{B}_j = X_j^2 Y_j'$, leading to $H_3 = \bar{x}$, which substantially simplifies the computation (see Sect. 5).

Substitute (3.1) into (2.17) and arrive at the classical **IP** with the second variation $\Xi_0[w]$ treated in the framework of Weierstrass' theory (see [3], Chap. 6). Analyzing the problem with functional $\Xi_2[w] = \Xi_0[w] + 2\mu\Xi_1[w]$,

$$\Xi_2[w] = \int_{t_2}^{t_1} \mathcal{H}(t, w, w') \mathrm{d}t, \quad \mathcal{H}(t, w, w') = H_1 w'^2 + H_2 w^2 + 2\mu H_3 w, \tag{3.3}$$

and the Lagrange multiplier μ, write ELE for the function $w(t)$ as an inhomogeneous Jacobi equation with BC given in (3.1)

$$(H_1 w')' - H_2 w = \mu H_3, \quad w(t_1) = w(t_2) = 0. \tag{3.4}$$

The point $t_2' \neq t_2$ is called *conjugate* to the point t_2, if (3.4) has a solution $\bar{w}(t)$ such that $\bar{w}(t_2) = \bar{w}(t_2') = 0$, but is not identically zero. According to Bolza [3], pp. 217–220, the following set of conditions is sufficient for the functional (3.3) to have a weak minimum for the solution $\bar{w}(t)$ of Eq. (3.4):

$$a) \quad H_1(t) > 0, \quad b) \quad \text{the interval } [t_2, t_1] \text{ contains no points conjugate to } t_2. \tag{3.5}$$

In fact, (3.5) provide a strong minimum because the Weierstrass function $\mathcal{E}(t, w, w', f) = \mathcal{H}(t, w, f) - \mathcal{H}(t, w, w') + (w' - f)\mathcal{H}_{w'}(t, w, w')$ for the functional $\Xi_2[w]$ in (3.3) is positive,

$$\mathcal{E}(t, w, w', f) = H_1 \left[f(t) - w'(t)\right]^2, \quad \text{for } f(t) \neq w'(t). \tag{3.6}$$

Weierstrass [27], p. 275, gave another version of conjugate points nonexistence condition. Assume that $\bar{w}_1(t)$ and $\bar{w}_2(t)$ are fundamental solutions of homogeneous Jacobi equation, then the particular solution $\mu\bar{w}_3(t)$ of inhomogeneous Jacobi equation (3.4) may be found by standard procedure

$$\bar{w}_3(t) = \bar{w}_2 \int^t \frac{\bar{w}_1 H_3}{H_1 \mathsf{Wr}}\, \mathrm{d}s - \bar{w}_1 \int^t \frac{\bar{w}_2 H_3}{H_1 \mathsf{Wr}}\, \mathrm{d}s, \quad \mathsf{Wr} = \bar{w}_1 \bar{w}_2' - \bar{w}_2 \bar{w}_1', \tag{3.7}$$

where Wr denotes the Wronskian for fundamental solutions. Find Wr assuming that $\bar{w}_1$ is known and the second fundamental solution reads $\bar{w}_2 = U(t)\bar{w}_1$. Substitute it into (3.4) with $\mu = 0$ and obtain

$$\frac{\mathrm{d}}{\mathrm{d}t}\left(H_1 \bar{w}_1^2 \frac{\mathrm{d}U}{\mathrm{d}t}\right) = 0, \quad \frac{\mathrm{d}U}{\mathrm{d}t} = \frac{g}{H_1 \bar{w}_1^2}, \quad \mathsf{Wr} = \bar{w}_1^2 \frac{\mathrm{d}U}{\mathrm{d}t} = \frac{g}{H_1}, \tag{3.8}$$

where g is an integration constant. The fundamental solutions w_j also can be expressed as $w_j = y'(\partial x/\partial \alpha_j) - x'(\partial y/\partial \alpha_j)$, $j = 1, 2$, where α_j denotes the integration constant emerging from ELE (see Bolza [3], p.219). Making use of expression for Wr in (3.7), we get

$$g\bar{w}_3 = \bar{w}_2 J_1 - \bar{w}_1 J_2, \quad g\bar{w}_3' = \bar{w}_2' J_1 - \bar{w}_1' J_2, \quad g\bar{w}_3'' = \bar{w}_2'' J_1 - \bar{w}_1'' J_2 + \frac{gH_3}{H_1},$$

where $J_k = \int^t H_3 \bar{w}_k \mathrm{d}s$. Following Weierstrass [27] introduce the matrix,

$$D(t_2, t') = \begin{pmatrix} \bar{w}_1(t_2) & \bar{w}_2(t_2) & \bar{w}_3(t_2) \\ \bar{w}_1(t') & \bar{w}_2(t') & \bar{w}_3(t') \\ J_1(t') - J_1(t_2) & J_2(t') - J_2(t_2) & J_3(t') - J_3(t_2) \end{pmatrix}. \tag{3.9}$$

Then the condition of nonexistence of conjugate points reads (see [27], p. 275),

$$\Delta(t_2, t') \neq 0, \quad t_2 < t' < t_1, \quad \Delta(t_2, t_1) = \det D(t_2, t_1). \tag{3.10}$$

Bolza in [3], p. 223, gave a more general condition of nonexistence of conjugate points,

$$\Delta(t'', t') \neq 0, \quad t_2 < t' < t'' < t_1, \tag{3.11}$$

making the Jacobi condition (3.5b) symmetric w.r.t. the endpoints t_2 and t_1. Write a determinant equation $\Delta(t_2, t_1) = 0$ as follows,

$$\begin{aligned} \Delta(t_2, t_1) = {} & I_3 \left[\bar{w}_1(t_2)\bar{w}_2(t_1) - \bar{w}_1(t_1)\bar{w}_2(t_2)\right] \\ & + \left[I_1 \bar{w}_2(t_1) - I_2 \bar{w}_1(t_1)\right] \bar{w}_3(t_2) + \left[I_2 \bar{w}_1(t_2) - I_1 \bar{w}_2(t_2)\right] \bar{w}_3(t_1). \end{aligned} \tag{3.12}$$

where $I_k = J_k(t_1) - J_k(t_2)$. If $\bar{w}_1(t)$ and $\bar{w}_2(t)$ are continuous functions, then equation $\Delta(t_2, t_1) = 0$ describes a continuous curve $D(t_2, t_1)$ of conjugated points.

Another important requirement is to guarantee that the extremal $\{\bar{x}(t), \bar{y}(t)\}$ does not intersect with the curves S_j. In the case of the PR, this requirement provides the meniscus existence condition given by the constant sign of $\eta(t_j, \tau_j^*)$. Define the lines $t_j = t_j^\bullet$ in $\{t_1, t_2\}$-plane where $\eta(t_j^\bullet, \tau_j^*) = 0$.

Consider a point $M_1 = (a, b)$ in the lower halfplane $\{t_2 < t_1\}$ and two more points: $M_2 = (a, a)$ and $M_3 = (b, b)$. Call a point M_1 the Jacobi point if the line M_1M_2 does not intersect both $D(t_2, t_1)$ and $t_2 = t_2^\bullet$, and M_1M_3 does not intersect both $D(t_2, t_1)$ and $t_1 = t_1^\bullet$. Define a set $\mathbb{J}(t_2, t_1)$ as a union of points M_1

$$\mathbb{J}(t_2,t_1)=\left\{(a,b)\;\middle|\;\begin{array}{ll}\Delta(t,a)\neq 0, & \Delta(b,t)\neq 0,\;\; t_2<b\le t\le a<t_1,\\ \eta(t_2,\tau_2^*)\neq 0, & t_2^\bullet<b\le t_2\le a<t_1,\\ \eta(t_1,\tau_1^*)\neq 0, & t_2<b\le t_1\le a<t_1^\bullet.\end{array}\right\} \tag{3.13}$$

representing an open domain in $\{t_1, t_2\}$-plane. Combining (3.5a, b) and (3.13) define a stability set as intersection set

$$\begin{aligned}\mathsf{Stab}_1(t_2,t_1) &= \mathbb{J}(t_2,t_1)\cap\mathbb{L}(t_2,t_1),\\ \mathbb{L}(t_2,t_1) &= \{(t_2,t_1)|H_1(t)>0,\; t\in[t_2,t_1]\},\end{aligned} \tag{3.14}$$

where the set $\mathbb{L}(t_2, t_1)$ comprises the points satisfying Legendre's criterion (3.5a).

4. Inhomogeneous boundary conditions: free endpoints

Consider the case when the extremal $\{\bar{x}(t), \bar{y}(t)\}$ is perturbed at the interval $[t_2, t_1]$ including both endpoints. The case of one free and one fixed endpoints will follow as a corollary. The non-integral term in (2.17) is fixed and in general case it does not vanish; the same is true for (2.20). It is worth to mention that any other BC, e.g., the Neumann BC $w'(t_j) = 0$ in [23] or mixed BC $g_1w'(t_j) + g_0w(t_j) = 0$ in [15], leads to changes in $u(t_j)$, $v(t_j)$ and requires variation of the non-integral term in (2.17).

From physical point of view, BC (2.13) requires that *the endpoints of perturbed meniscus* $\{\bar{x}+u, \bar{y}+v\}$ *always belong to the solid surfaces*. These claims are justified from mathematical standpoint:

- The Jacobi equation (3.4) for perturbation w admits no more than two BC.
- The perturbed meniscus $\{\bar{x} + u, \bar{y} + v\}$ may not provide the extremum for $W[x, y]$ even if $\{u, v\}$ do provide the extremum for $\delta^2W[x, y]$.

Following an ideology of stability theory, we have to find when δ^2W is positive definite in vicinity of the extremal curve constrained by (2.2). Since the only varying part in (2.20) is the functional $\Xi_0[w]$, this brings us to **IP-2** with one indeterminate function $w(t)$: Find the extremal $\bar{w}(t)$ providing $\Xi_0[w]$ to be positive definite in vicinity of $\bar{w}(t)$ and preserving $\Xi_1[w]$. Inhomogeneity of BC requires to answer two questions:

When is $\Xi_0[w]$ *positive definite in vicinity of* $\bar{w}(t)$ *for the fixed* $\delta\tau_j$*?* (4.1)

When does $\Xi_0[\bar{w}]$ *reach a positive value as a function of displacements* $\delta\tau_j$*?* (4.2)

Consider the necessary conditions for functional $\Xi_0[w]$ to be positive definite in vicinity of extremal perturbation $\bar{w}(t)$ for the fixed $\delta\tau_j$ and preserving $\Xi_1[w]$. Let us prove that they coincide with those conditions (3.5) for the functional $E[x, y]$ to be positive definite in vicinity of extremal solution $\{\bar{x}(t), \bar{y}(t)\}$ for the fixed endpoints and preserving $V[x, y]$.

For this purpose, we ignore a fact that $\Xi_0[w]$ is a second variation, satisfying the relations (2.18), and instead, we treat the analysis of (2.18) as independent problem. Represent w in a vicinity of extremal perturbation $\bar{w}$,

$$w(t)=\bar{w}(t)+\varepsilon(t),\quad \varepsilon(t_1)=\varepsilon(t_2)=0,\quad \Xi_1[\varepsilon]=\int_{t_2}^{t_1}H_3\varepsilon\mathrm{d}t=0, \tag{4.3}$$

where a perturbation ε preserves both BC (2.13) and the constraint (3.2). Find the first and second variations of functional $\Xi_2[w]$ defined in (3.3),

$$\delta\Xi_2[w]=2\int\limits_{t_2}^{t_1}\left(-\left(H_1\bar{w}'\right)'+H_2\bar{w}+\mu H_3\right)\varepsilon\mathrm{d}t,\quad \delta^2\Xi_2[w]=\int\limits_{t_2}^{t_1}\left(H_1\varepsilon'^2+H_2\varepsilon^2\right)\mathrm{d}t.$$

The first variation $\delta\Xi_2[w]$ vanishes at the extremal $\bar{w}$ satisfying the inhomogeneous Jacobi equation (3.4). Regarding the second variation $\delta^2\Xi_2[w]$, it completely coincides with $\Xi_0[w]$ as well as BC and volume constraint (4.3) is coinciding with similar BC (3.1) and constraint (3.2) in the **IP** with fixed endpoints (Sect. 3). This coincidence implies the necessary conditions (3.5) for $\Xi_0[w]$ to be positive definite in vicinity of extremal $\bar{w}$ for the fixed $\delta\tau_j$.

Consider (4.2) and write a general solution $\bar{w}$ of equation (3.4) built upon the fundamental solutions $\bar{w}_1,\bar{w}_2$ of homogeneous equation, and particular solution $\bar{w}_3$ of inhomogeneous equation,

$$\bar{w}(t)=C_1\bar{w}_1(t)+C_2\bar{w}_2(t)+\mu\bar{w}_3(t). \tag{4.4}$$

Inserting (4.4) into (2.13) and into constraint (3.2), we obtain three linear equations,

$$\bar{w}_1(t_j)C_1+\bar{w}_2(t_j)C_2+\bar{w}_3(t_j)\mu=\bar{w}(t_j),\quad I_1C_1+I_2C_2+I_3\mu=0, \tag{4.5}$$

which are uniquely solvable (see [3], p. 220) if $\Delta(t_2,t_1)\neq 0$ and have nonzero solutions when at least one of $\bar{w}(t_j)$ is nonzero,

$$C_j=m_{j1}\delta\tau_1+m_{j2}\delta\tau_2,\quad j=1,2,\quad \mu=m_{31}\delta\tau_1+m_{32}\delta\tau_2. \tag{4.6}$$

Substitute (4.6) into (4.5) and find two equations with matrix $D(t_2,t_1)$ in (3.9),

$$D(t_2,t_1)\mathbf{M}_j=\mathbf{N}_j,\quad \mathbf{M}_j=\begin{pmatrix}m_{1j}\\ m_{2j}\\ m_{3j}\end{pmatrix},\quad \mathbf{N}_1=\begin{pmatrix}0\\ \eta_1\\ 0\end{pmatrix},\quad \mathbf{N}_2=\begin{pmatrix}\eta_2\\ 0\\ 0\end{pmatrix},$$

where $\eta_j=\eta(t_j,\tau_j^*)$ and $\bar{w}_i(t_j)=\bar{w}_{ij}$. Then $m_{j1}=\eta_1\beta_{j1}/\Delta$, $m_{j2}=\eta_2\beta_{j2}/\Delta$,

$$\begin{aligned}&\beta_{11}=I_3\bar{w}_{22}-I_2\bar{w}_{32},\quad \beta_{21}=I_1\bar{w}_{32}-I_3\bar{w}_{12},\quad \beta_{31}=I_2\bar{w}_{12}-I_1\bar{w}_{22},\\ &\beta_{12}=I_2\bar{w}_{31}-I_3\bar{w}_{21},\quad \beta_{22}=I_3\bar{w}_{11}-I_1\bar{w}_{31},\quad \beta_{32}=I_1\bar{w}_{21}-I_2\bar{w}_{11}.\end{aligned}$$

Substituting (4.6) into (4.4) represents $\bar{w}(t)$ as follows

$$\bar{w}(t)=A_1(t)\delta\tau_1+A_2(t)\delta\tau_2,\quad A_j(t)=\frac{\eta_jB_j(t)}{\Delta(t_2,t_1)},\quad B_j(t)=B_j(t,t_2,t_1), \tag{4.7}$$

$$B_1(t)=-\begin{vmatrix}\bar{w}_1(t) & \bar{w}_2(t) & \bar{w}_3(t)\\ \bar{w}_1(t_2) & \bar{w}_2(t_2) & \bar{w}_3(t_2)\\ I_1 & I_2 & I_3\end{vmatrix},\quad B_2(t)=\begin{vmatrix}\bar{w}_1(t) & \bar{w}_2(t) & \bar{w}_3(t)\\ \bar{w}_1(t_1) & \bar{w}_2(t_1) & \bar{w}_3(t_1)\\ I_1 & I_2 & I_3\end{vmatrix}.$$

According to (2.13), we have $B_1(t_2)=B_2(t_1)=0$, $B_j(t_j)=\Delta(t_2,t_1)$, and its expression is given in (3.12). Direct calculation of determinant's derivatives gives

$$\begin{aligned}H_1(t_2)B_1'(t_2)&=-H_1(t_1)B_2'(t_1)=I_1(t_1)I_2(t_2)-I_1(t_2)I_2(t_1)+gI_3,\\ gB_1'(t_1)&=\left[I_2\bar{w}_1(t_2)-I_1\bar{w}_2(t_2)\right]\left[I_2\bar{w}_1'(t_1)-I_1\bar{w}_2'(t_1)\right]\\ &\quad -H_1(t_1)B_2'(t_1)[\bar{w}_1(t_2)\bar{w}_2'(t_1)-\bar{w}_2(t_2)\bar{w}_1'(t_1)],\\ gB_2'(t_2)&=\left[I_2\bar{w}_1(t_1)-I_1\bar{w}_2(t_1)\right]\left[I_2\bar{w}_1'(t_2)-I_1\bar{w}_2'(t_2)\right]\\ &\quad -H_1(t_2)B_1'(t_2)[\bar{w}_1(t_1)\bar{w}_2'(t_2)-\bar{w}_2(t_1)\bar{w}_1'(t_2)],\end{aligned} \tag{4.8}$$

where $B_j'(t_k) \equiv \mathrm{d}B_j(t,t_2,t_1)/\mathrm{d}t$ computed at $t=t_k$. Formula (2.17) together with Eq. (3.4) allows to express $\delta^2 W[x,y]$ in a simple form. Multiplying (3.4) by $\bar{w}$ and integrating by parts, we obtain

$$\int_{t_2}^{t_1} \left(H_1(t)\bar{w}'^2(t) + H_2(t)\bar{w}^2(t)\right) \mathrm{d}t - H_1(t)\bar{w}(t)\bar{w}'(t)|_{t_2}^{t_1} = 0.$$

Combining the last equality with (2.20) and (2.21), we arrive at

$$\delta^2 W = \frac{1}{2}\left(H_1\bar{w}\bar{w}' + Lu^2 + 2Muv + Nv^2\right)|_{t_2}^{t_1} + \xi_1(\delta\tau_1)^2 - \xi_2(\delta\tau_2)^2, \tag{4.9}$$

where ξ_j defined in (2.19). Substitute (2.12, 4.7) into (4.9) and using (4.8), we obtain

$$\delta^2 W = Q_{11}\left(\delta\tau_1\right)^2 + 2Q_{12}\delta\tau_1\delta\tau_2 + Q_{22}\left(\delta\tau_2\right)^2, \tag{4.10}$$

$$\begin{aligned} Q_{11}(t_2,t_1) &= \frac{\eta_1^2 P_{11}}{2\Delta} + K_1, \qquad & P_{11} &= H_1(t_1)B_1'(t_1),\\ Q_{22}(t_2,t_1) &= \frac{\eta_2^2 P_{22}}{2\Delta} - K_2, \qquad & P_{22} &= -H_1(t_2)B_2'(t_2),\\ Q_{12}(t_2,t_1) &= \frac{\eta_1\eta_2 P_{12}}{2\Delta}, \qquad & P_{12} &= P_{21} = H_1(t_1)B_2'(t_1), \end{aligned} \tag{4.11}$$

where $\eta_j = \eta(t_j,\tau_j^*)$ and $K_j = K_j(t_j,\tau_j^*)$ are defined in (2.13) and (2.21), respectively.

Using BC (2.11): $\bar{x}(t_j) = X(\tau_j^*)$, $\bar{y}(t_j) = Y(\tau_j^*)$, the matrix elements Q_{ij} may be represented as functions of t_2, t_1 only. Thus, we arrive at the main result of this section: positiveness of the second variation $\delta^2 W$ in (4.10) as a quadratic form in variables $\delta\tau_1, \delta\tau_2$.

Theorem 4.1. *Let $Q_{ij}(t_2,t_1)$ be given in accordance with (2.21, 3.12, 4.8 and 4.11). Then $\delta^2 W$ is positive definite if the following inequalities hold,*

$$Q_{11}(t_2,t_1) \geq 0, \quad Q_{22}(t_2,t_1) \geq 0, \quad Q_{33}(t_2,t_1) = Q_{11}Q_{22} - Q_{12}^2 \geq 0. \tag{4.12}$$

One of the two first inequalities in (4.12) is redundant, but we leave it for the symmetry considerations. Inequalities (4.12) provide an answer to the question (4.2). Define three different sets $\mathbb{Q}_j(t_2,t_1)$

$$\mathbb{Q}_j(t_2,t_1) := \{(a,b) \mid (a,b) \in \{t_2 < t_1\}, \quad Q_{jj}(t_2,t_1) \geq 0\}, \tag{4.13}$$

and the intersection set $\mathbb{Q}(t_2,t_1) := \mathbb{Q}_1(t_2,t_1) \cap \mathbb{Q}_2(t_2,t_1) \cap \mathbb{Q}_3(t_2,t_1)$.

Summarizing answers to both questions (4.1, 4.2) we conclude that the necessary conditions of stability of extremal $\bar{w}(t)$ with BC comprise (3.5), (3.10), (3.14) and (4.11):

$$\mathsf{Stab}_2(t_2,t_1) = \mathsf{Stab}_1(t_2,t_1) \cap \mathbb{Q}(t_2,t_1), \quad \mathsf{Stab}_2(t_2,t_1) \subseteq \mathsf{Stab}_1(t_2,t_1). \tag{4.14}$$

The conditions (4.12) cannot determine the extremal solution stability in case when the determinant Q_{33} in (4.12) vanishes. Indeed, we have in (4.10)

$$\delta^2 W = \left(\sqrt{Q_{11}}\delta\tau_1 + \sqrt{Q_{22}}\delta\tau_2\right)^2, \quad Q_{33}(t_2,t_1) = 0. \tag{4.15}$$

Thus, there exists a non-empty set of perturbations $\delta\tau_1, \delta\tau_2$ such that $\sqrt{Q_{11}}\delta\tau_1 + \sqrt{Q_{22}}\delta\tau_2 = 0$, which does not affect the second variation, i.e., $\delta^2 W = 0$. This limitation of the Weierstrass representation may be resolved by studying the higher variations, necessarily including both terms $\delta^3 W$ and $\delta^4 W$, which is beyond the scope of the present manuscript.

Consider two menisci related by symmetry reflection $t_2 \to -t_1, t_1 \to -t_2$ w.r.t. a midline between two solids and normal to the curve $\{\bar{x}(t), \bar{y}(t)\}$ at the point $t=0$ (or to continuation of curve if $0 \notin [t_2,t_1]$) as shown in Fig. 2.

It is easy to conclude that the stability conditions (4.12) serve for both menisci simultaneously,

$$Q_{ii}(-t_1,-t_2) = Q_{jj}(t_2,t_1), \quad i \neq j = 1,2; \quad Q_{12}(-t_1,-t_2) = Q_{12}(t_2,t_1). \tag{4.16}$$

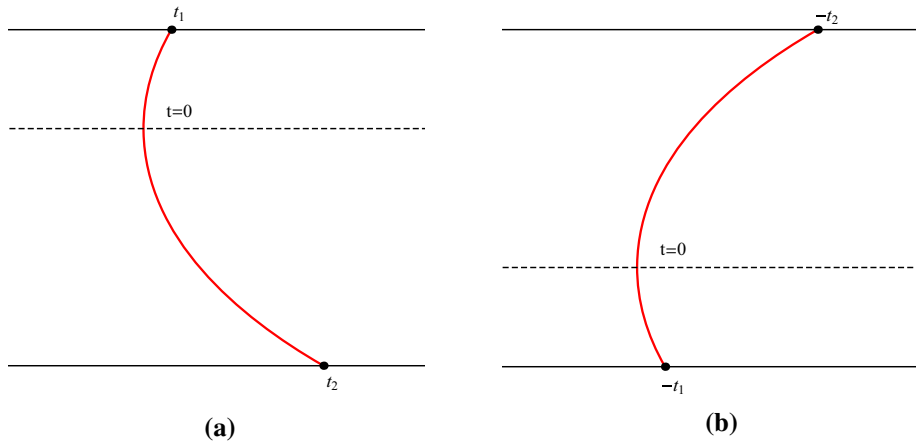

FIG. 2. Sketches of menisci between two plates showing the endpoints **a** t_1, t_2 and **b** $-t_2, -t_1$

Consider a symmetric setup: $t_1 = -t_2 = t$, when two solid bodies are similar and separated by a reflection plane located in the midpoint of the meniscus at $t = 0$. Then due to (4.16), the necessary conditions (4.12) read

$$Q_{11}(-t,t) = Q_{22}(-t,t) \geq 0, \quad Q_{33}(-t,t) = Q_{11}^2(-t,t) - Q_{12}^2(-t,t) \geq 0. \tag{4.17}$$

Expression (4.10) and conditions (4.12) encompass the case when the extremal curve is perturbed at interval $[t_2, t_1]$ including only one endpoint (say, t_1), while another is left fixed. Here we have $\delta^2 W = Q_{11} \left(\delta\tau_1\right)^2$, $Q_{11}(t_2, t_1) \geq 0$.

5. Application to the problem of liquid bridges

Apply our approach to study the stability of axisymmetric LB between solid bodies in the absence of gravity. The axial symmetry of bodies is assumed along z-axis (see Fig. 3). The shapes of meniscus $\{r(\phi), z(\phi)\}$ and two solid bodies $\{R_j(\psi_j), Z_j(\psi_j)\}$ are given in cylindrical coordinates, i.e., the following correspondence holds, $x \to r$, $y \to z$, $X_j \to R_j$, $Y_j \to Z_j$, $t \to \phi$, $\tau_j \to \psi_j$.

The filling angle ψ_j along the j solid–liquid interface is chosen to satisfy $0 \leq \psi_j \leq \infty$ for unbounded solid bodies (semispace with planar boundary, paraboloid, catenoid) and $0 \leq \psi_j \leq$ const for bounded solid bodies (e.g., for sphere, prolate and oblate ellipsoids const $= \pi$).

The functional W and its integrands in (2.4) read

$$\begin{aligned} W &= \int_{\phi_2}^{\phi_1} F(r, r', z, z') \mathrm{d}\phi - \sum_{j=1}^{2} (-1)^j \int_0^{\psi_j^*} G_j \mathrm{d}\psi_j, \\ F &= \left[\gamma_{lv} \sqrt{r'^2 + z'^2} - \frac{\lambda r z'}{2} \right] r, \\ G_j &= \left[\frac{\lambda R_j Z_j'}{2} - (-1)^j (\gamma_{ls_j} - \gamma_{vs_j}) \sqrt{R_j'^2 + Z_j'^2} \right] R_j, \end{aligned} \tag{5.1}$$

where coefficients γ_{lv}, γ_{ls_j} and γ_{vs_j}, $j = 1, 2$, describe surface energy density at three interfaces: liquid–vapor, solid–vapor and solid–liquid for the upper ($j = 1$) and lower ($j = 2$) solid bodies. The two ELE (2.14) are reduced to a single YLE

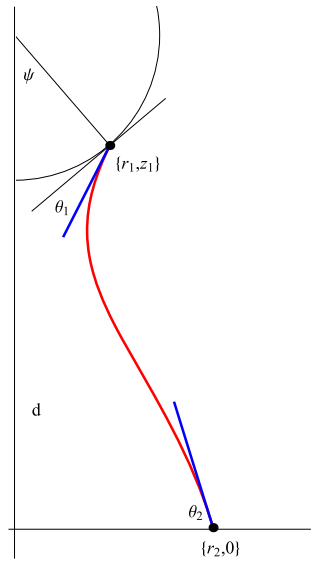

FIG. 3. A sketch of meniscus between plane and sphere showing the contact angles θ_1, θ_2, filling angle ψ and coordinates of the endpoints

$$2H = \frac{z'}{r(r'^2+z'^2)^{1/2}} + \frac{z''r' - z'r''}{(r'^2+z'^2)^{3/2}}, \quad H = \frac{\lambda}{2\gamma_{lv}}, \tag{5.2}$$

where H stands for the meniscus mean curvature. The transversality conditions (2.15) are known as the Young relations for the contact angle θ_j of the meniscus with the j-th solid body: $\cos\theta_j + (\gamma_{ls_j} - \gamma_{vs_j})/\gamma_{lv} = 0$. According to (2.13) the quantity $\eta_j = \eta(\phi_j, \psi_j^*)$ reads,

$$\eta_j = \bar{z}'(\phi_j)R'(\psi_j^*) - \bar{r}'(\phi_j)Z'(\psi_j^*). \tag{5.3}$$

Define a contact angle θ_j between meniscus and solid body as follows

$$\theta_j = (-1)^{j-1}\left(\arctan\frac{\bar{z}'(\phi_j)}{\bar{r}'(\phi_j)} - \arctan\frac{Z'(\psi_j^*)}{R'(\psi_j^*)}\right), \tag{5.4}$$

where $0 \le \arctan(\bar{z}'/\bar{r}'),\ \arctan(Z'/R') \le \pi$. The contact angle θ_j vanishes when $\bar{z}'/\bar{r}' = Z'/R'$, i.e., $\eta_j = 0$, which manifests meniscus' nonexistence at a critical angle $\phi_j^\bullet$ in accordance with (3.13)

$$\bar{z}'(\phi_j^\bullet)R'(\psi_j^*) - \bar{r}'(\phi_j^\bullet)Z'(\psi_j^*) = 0, \qquad \bar{r}(\phi_j^\bullet) - R(\psi_j^*) = 0. \tag{5.5}$$

Rescale the integrands in (2.4) by $2\gamma_{lv}|H|$ and deal henceforth with expressions,

$$F = \left[\sqrt{r'^2+z'^2} - \frac{S_H}{2}rz'\right]r, \tag{5.6}$$

$$G_j = \left[\frac{S_H}{2}R_jZ_j' + (-1)^j\cos\theta_j\sqrt{R_j'^2+Z_j'^2}\right]R_j,$$

where $S_H = \operatorname{sign} H$. Direct calculation in (2.21) gives an expression for K_j,

$$K_j = U_j\eta_j, \quad U_j = -\frac{R_j}{2\sqrt{\bar{r}_j'^2+\bar{z}_j'^2}}\left(\frac{\bar{z}_j''R_j' - \bar{r}_j''Z_j'}{\bar{r}_j'^2+\bar{z}_j'^2} - \frac{Z_j''R_j' - R_j''Z_j'}{R_j'^2+Z_j'^2}\right), \tag{5.7}$$

where $\bar{f}_j' = \bar{f}'(\phi_j)$, $\bar{f}_j'' = \bar{f}''(\phi_j)$. Combining (5.7, 4.11) find $Q_{ij}(\phi_2, \phi_1)$,

$$Q_{11}=\eta_1\left(\frac{\eta_1 P_{11}}{2\Delta}+U_1\right),\quad Q_{22}=\eta_2\left(\frac{\eta_2 P_{22}}{2\Delta}-U_2\right),\quad Q_{12}=\frac{\eta_1\eta_2 P_{12}}{2\Delta},\tag{5.8}$$

that results in $Q_{33}\propto\eta_1\eta_2$ and according to (4.16) we have $U_j(-\phi,\psi^*)=U_j(\phi,\psi^*)$. Thus, stability domain $\mathsf{Stab}_2(\phi_1,\phi_2)$ of liquid meniscus of any type has boundaries including meniscus nonexistence lines $\phi_j=\phi_j^\bullet$ given by (5.5).

Find formulas for H_j in (3.4) by substituting (5.6) into (2.18, 3.2) and obtain

$$\begin{gathered}H_1=\frac{\bar r}{\left(\bar r'^2+\bar z'^2\right)^{3/2}},\quad H_2=\frac{\left(H_1\bar r''\right)'}{\bar r'},\quad H_3=\bar r,\\ \left(H_1 w'\right)'\bar r'-\left(H_1\bar r''\right)' w=\mu\bar r'\bar r.\end{gathered}\tag{5.9}$$

Fundamental solutions of Eq. (5.9) read,

$$\bar w_1=\bar r'(\phi),\quad \bar w_2=E(\phi)\bar r'(\phi),\quad E(\phi)=g\int^{\phi}\frac{\mathrm{d}t}{H_1\bar r'^2}=g\int^{\phi}\frac{\left(\bar r'^2+\bar z'^2\right)^{3/2}\mathrm{d}t}{\bar r'^2\bar r}.$$

5.1. Liquid bridges with zero curvature

For $H=0$ the first Delaunay's type, *catenoid* (Cat) appears from (5.2),

$$\bar r=\sec\phi,\quad \bar z=\ln\frac{\cos\phi}{1-\sin\phi}+C,\quad \frac{\bar z'}{\bar r'}=\cot\phi,\quad \bar r'^2+\bar z'^2=\bar r^4,\tag{5.10}$$

where C is the constant determined from the BC. Entries in (2.17) read,

$$\begin{gathered}H_1=\frac{1}{\bar r^5},\quad H_2=-4\frac{\bar r^2-1}{\bar r^5},\\ L=\frac{\bar r^3\,\bar r'-\bar z'\,\bar z''}{\bar r^5},\quad N=-\frac{\bar r'\,\bar r''}{\bar r^5},\quad M=\frac{\bar z'\,\bar r''}{\bar r^5}.\end{gathered}\tag{5.11}$$

Note that $H_1(\phi)$ is always positive; therefore, the set $\mathbb{L}(\phi_1,\phi_2)$ is given by the whole lower halfplane $\{\phi_2<\phi_1\}$. The Jacobi equation (5.9) in this case reads

$$w''-5w'\tan\phi+4w\tan^2\phi=\mu\sec^6\phi.$$

Its fundamental and particular solutions and auxiliary functions read,

$$\begin{aligned}&\bar w_1=\tan\phi\,\sec\phi,\quad \bar w_2=\sec^2\phi-T(\phi)\bar w_1,\\ &\bar w_3=-\frac{\sec^4\phi}{2}+\frac{3}{4}\bar w_1\left[T(\phi)+\bar w_1\right],\quad T(\phi)=\ln\left(\tan\phi+\sec\phi\right),\\ &J_1(\phi)=\frac{\sec^2\phi}{2},\quad J_2(\phi)=\frac{T(\phi)}{4}\left[3-4J_1(\phi)\right]+\frac{3}{4}\bar w_1,\\ &J_3(\phi)=\frac{3T(\phi)}{32}\left[8J_1(\phi)-5\right]+\frac{\bar w_1}{32}\left[4J_1(\phi)-15\right].\end{aligned}\tag{5.12}$$

The determinant $\Delta_{cat}(\phi_1,\phi_2)=\Delta_{cat}$ is given by

$$\frac{32\Delta_{cat}}{K_{12}}=T_{12}(7M_3-2M_5-6M_1)-[3T_{12}^2-3L_2+4L_4]J_{12}+(L_2-2)(2L_2-3)K_{12},$$

where

$$\begin{aligned}&T_{12}=T(\phi_1)-T(\phi_2),\quad J_{12}=\tan\phi_1\tan\phi_2,\quad K_{12}=\sec\phi_1\sec\phi_2,\\ &L_n=\sec^n\phi_1+\sec^n\phi_2,\quad M_n=\tan\phi_1\sec^n\phi_2-\tan\phi_2\sec^n\phi_1.\end{aligned}$$

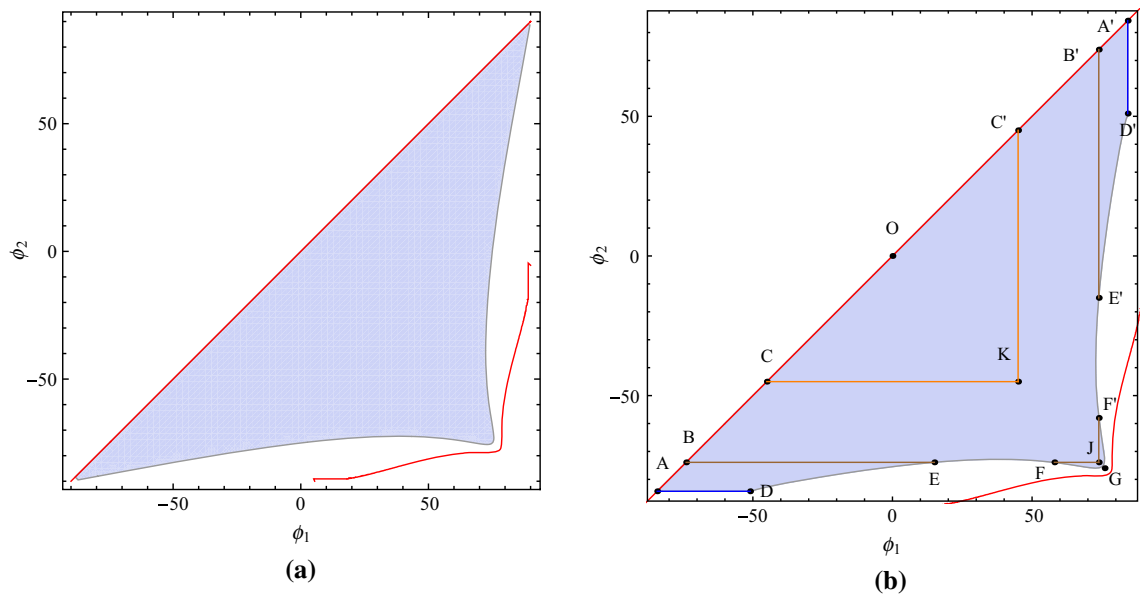

FIG. 4. **a** Stability diagram (SD) for Cat menisci between two plates is shaded in *gray*; its boundary coincides with the curve given by (5.13). **b** The SD for Cat menisci between two equal spheres are represented by interiors of polygons: $A = 100$, {OCBADEFGF'E'D'A'B'C'O}, $\phi^\bullet(1, 100) = 84.3°$; $A = 13$, {OCBEFJF'E'A'B'C'O}, $\phi^\bullet(1, 13) = 73.9°$; $A = 4$, {OCKC'O} $\phi^\bullet(1, 4) = 60°$. The *red curves* show the location of conjugate points while the *blue lines* show the location of points where $\eta(\phi_j^\bullet, \psi_j^*) = 0$, $\sec\phi_j^\bullet = 100 \sin\psi_j^*$ (color figure online)

Matrix P_{ij} calculated from (4.11) is too cumbersome to be presented here. Functions $\eta(\phi_j, \psi_j^*)$ and $K(\phi_j, \psi_j)$ are calculated substituting (5.10) into (5.3, 5.7).

5.1.1. Cat meniscus between two plates. The Cat with given endpoints on two solid plates exists for arbitrary contact angles θ_j. Parametrization of plates and relations between ϕ_j and θ_j read (see Fig. 4a)

$$R_j = A\psi_j,\ Z_j = d_j,\ \theta_j = \frac{\pi}{2} + (-1)^j\phi_j, \qquad \eta_j = A\sec\phi_j,\ 2K_j = -A^2\sin\phi_j\cos^2\phi_j.$$

By (5.5) the critical angles $\phi_j^\bullet$ read: $\phi_j^\bullet = (-1)^{j+1}\pi/2$ that makes every point of infinite plates (at the distance $d = d_1 - d_2$) attainable by Cat meniscus.

In Fig. 4a, the red curve determines the boundaries of $\mathsf{Stab}_1(\phi_1, \phi_2)$ defined in (3.14), while the lower boundary of stability domain gives the boundaries of $\mathsf{Stab}_2(\phi_1, \phi_2)$ defined in (4.14). Numerical calculations show a nice coincidence with boundaries found in the framework of Vogel's approach in [29],

$$5\int_{\phi_1}^{\phi_2}\cos^{-5}t\,\mathrm{d}t\cdot\int_{\phi_1}^{\phi_2}\cos^{-1}t\,\mathrm{d}t = 9\left(\int_{\phi_1}^{\phi_2}\cos^{-3}t\,\mathrm{d}t\right)^2. \tag{5.13}$$

In symmetric setup (4.17) Cat, meniscus between two plates is stable if $\theta \geq 14.97^o$.

5.1.2. Cat meniscus between two ellipsoids. Consider Cat meniscus between two axisymmetric ellipsoids given by equation $R_j^2 + (Z_j - g_j)^2\,\epsilon_j^{-2} = A^2$, $\epsilon_j > 0$, where ϵ_j stands for anisotropy parameter and $\{0, g_j\}$ denotes coordinates of the j-th ellipsoid center. Ellipsoids may be specified as prolate ($\epsilon_j > 1$) and oblate ($\epsilon_j < 1$). The upper and lower ellipsoids are separated by distance $d = g_1 - g_2 - A(\epsilon_1 + \epsilon_2)$ and given parametrically,

$$R_j = A\sin\psi_j, \quad Z_j = g_j + (-1)^j A\epsilon_j \cos\psi_j,$$
$$\eta_j = \frac{\sqrt{A^2\cos^2\phi_j - 1} + (-)^j \epsilon_j \tan\phi_j}{\cos^2\phi_j},$$
$$K_j = -\frac{\eta_j \cos\phi_j}{2}\left(\eta_j \sin\phi_j \cos^3\phi_j + (-1)^j\epsilon_j\left[1 + \frac{1}{\cos^2\phi_j + \epsilon_j^2\sin^2\phi_j}\right]\right).$$

According to (5.4), the contact angles are given by

$$\theta_j = \frac{\pi}{2} + (-1)^j\phi_j - \arctan\frac{\epsilon_j}{\sqrt{A^2\cos^2\phi_j - 1}}.$$

By (5.5) the critical angles $\phi_j^\bullet = \phi_j^\bullet(\epsilon_j, A)$ are given by equation,

$$A^2\cos^4\phi_j^\bullet + (\epsilon_j^2 - 1)\cos^2\phi_j^\bullet - \epsilon_j^2 = 0,$$
$$\phi_1^\bullet(1, A) = -\phi_2^\bullet(1, A) = \arccos\frac{1}{\sqrt{A}}, \tag{5.14}$$

where $\epsilon_j = 1$ stands for two equal spheres. This makes the areas, attainable by Cat stable meniscus on the spheres, substantially limited. Figure 4b shows stability diagrams (SD) of Cat menisci between two equal spheres of different radii. Decrease of A reduces the stability domain $\mathsf{Stab}_2(\phi_1, \phi_2)$ caused by non-planar solid bodies and decrease of $\phi_j^\bullet$. For $A < 11.7$ the domain $\mathsf{Stab}_2(\phi_1, \phi_2)$ is a right isosceles triangle $\{OCKC'O\}$, otherwise the domain has curvilinear boundaries.

5.1.3. Cat meniscus between other solid bodies. The theory of LB stability with free CL developed in Sect. 4 can be applied to arbitrary pair of axisymmetric solid bodies. Here we study another pair, two paraboloids. Consider the Cat meniscus between two convex parts of axisymmetric solid bodies,

$$R_j = A\psi_j, \quad Z_j = g_j + (-1)^{j+1}AC_j a_j(\psi_j/a_j)^{\nu_j}, \quad a_j,\ \nu_j,\ C_j,\ A > 0. \tag{5.15}$$

For $\nu_j > 1$ the surface is smooth at $\psi_j = 0$, otherwise it has a singularity point. The case $\nu_j = 1$ represents a conic surface. The critical angles $\phi_j^\bullet$ are given by relations,

$$\nu_j C_j \tan\phi_j^\bullet = \left(a_j A\cos\phi_j^\bullet\right)^{\nu_j - 1}, \ \nu_j > 1; \quad \cot\phi_j^\bullet = C_j, \ \nu_j = 1.$$

When Cat meniscus connects solid bodies of different shapes, the stability domain loses its symmetry w.r.t. the line $\phi_1 + \phi_2 = 0$, thus breaking an equality $\phi_1^\bullet = -\phi_2^\bullet$ for critical angles. This can be seen in the setup of meniscus between solid sphere and plate at Fig. 5, for which according to (5.14) we have,

$$\phi_1^\bullet(1, A) = \arccos\frac{1}{\sqrt{A}}, \quad \phi_2^\bullet(0, A) = -\arccos\frac{1}{A}.$$

6. Liquid bridges with nonzero curvature

For $H \neq 0$ Eq. (5.2) is solved in elliptic integrals of the first F and the second E kind. Here we choose a parametrization similar to that used in [10,12],

$$\bar r(\phi) = \sqrt{1 + B^2 + 2B\cos(S_H\phi)},$$
$$\bar z(\phi) = M(S_H\phi, B) - M(S_H\phi_2, B) + Z_2(\psi_2), \tag{6.1}$$
$$M(\phi, B) = (1 + B)E(\phi/2, m) + (1 - B)F(\phi/2, m), \quad m^2 = \frac{4B}{(1 + B)^2},$$

and provide a correct sign for H in (5.2) for two different types of Nod menisci with $S_H = \pm 1$ defined in (5.6). Here m stands for modulus of elliptic integral. The expression for B is given by

$$B^2 + 2B\cos(S_H\phi_1) + 1 = R_1^2(\psi_1).$$

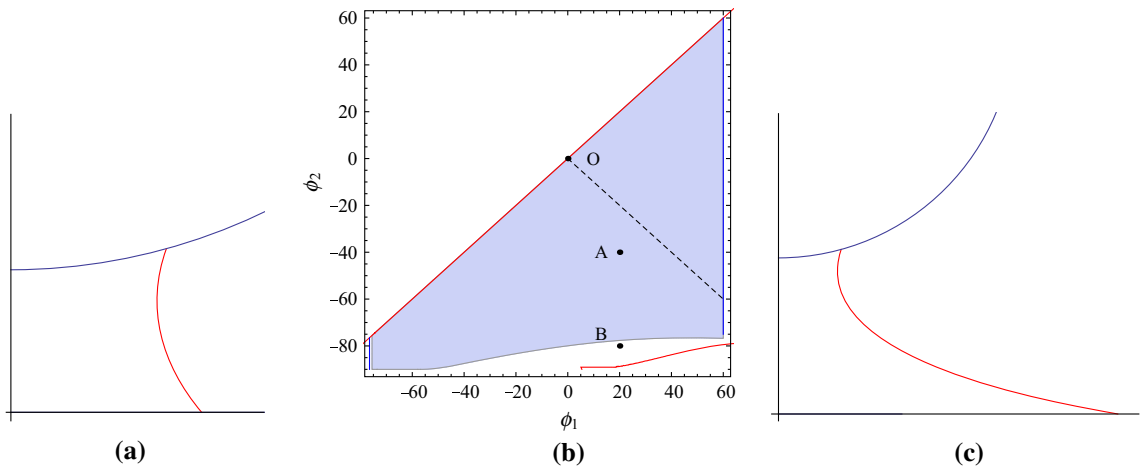

FIG. 5. The SD **b** for Cat menisci between solid plate and sphere, $A = 4$, is not symmetric w.r.t. the *dashed* line $\phi_1 + \phi_2 = 0$. The critical angles are $\phi_1^\bullet(1,4) = 60°$, $\phi_2^\bullet(0,4) = -75.5°$. Points A and B mark **a** stable $\phi_1 = 20°, \phi_2 = -40°$, and **c** unstable $\phi_1 = 20°, \phi_2 = -80°$, menisci, respectively

The derivatives $\bar{r}', \bar{r}''$ and $\bar{z}', \bar{z}''$ satisfy the relationships

$$\begin{aligned} &\frac{\bar{r}'}{B} = -\frac{\sin(S_H\phi)}{S_H\,\bar{r}}, \quad \frac{\bar{r}''}{B} = \frac{\bar{r}'\sin(S_H\phi)}{S_H\,\bar{r}^2} - \frac{\cos(S_H\phi)}{\bar{r}}, \\ &\bar{z}' = \frac{1 + B\cos(S_H\phi)}{S_H\bar{r}}, \quad \bar{z}'' = \bar{r}'\left(S_H - \frac{\bar{z}'}{\bar{r}}\right). \end{aligned} \tag{6.2}$$

Formulas (6.1) describe four Delaunay's types [5] of surfaces of revolution with constant H: *cylinder* (Cyl), $B = 0$, *unduloid* (Und), $B < 1$, *sphere* (Sph), $B = 1$, and *nodoid* (Nod), $B > 1$. Entries in (2.17) read,

$$H_1 = H_3 = \bar{r}, \quad H_2 = -\left(\bar{r} + 2\bar{r}''\right), \quad L = \bar{r}' - \bar{z}'\bar{z}''\bar{r}, \quad N = -\bar{r}'\bar{r}''\bar{r}, \quad M = \bar{z}'\bar{r}''\bar{r}.$$

Note that $\bar{r}'^2 + \bar{z}'^2 = 1$, and H_1 are positive as in Sect. 5.1. Equation (5.9) reads

$$w'' - \frac{B\sin\phi}{\bar{r}^2}w' + \left(1 - \frac{2B\cos\phi}{\bar{r}^2} - \frac{2B^2\sin^2\phi}{\bar{r}^4}\right)w = \mu. \tag{6.3}$$

Its fundamental and particular solutions and corresponding auxiliary functions read:

$$\begin{aligned} &\bar{w}_1 = \frac{\sin\phi}{\bar{r}}, \quad \bar{w}_2 = \cos\phi + (1+B)M_1\bar{w}_1, \quad \bar{w}_3 = 1 + (1+B)M_2\bar{w}_1, \\ &J_1 = -\cos\phi, \quad \eta_j = \frac{1}{\bar{r}(\phi_j)}\left[S_H(1 + B\cos\phi_j)R_j'(\psi_j^*) + B\sin\phi_j Z_j'(\psi_j^*)\right], \\ &J_2 = \bar{r}\sin\phi + (1+B)(J_1M_1 + M_2), \; J_3 = (1+B)\left[2E\left(\frac{\phi}{2}, m\right) + J_1M_2 + M_1\right] \\ &M_1(\phi, m) = E\left(\frac{\phi}{2}, m\right) - F\left(\frac{\phi}{2}, m\right) + M_2, \quad M_2(\phi, m) = \frac{m^2}{2}F\left(\frac{\phi}{2}, m\right). \end{aligned} \tag{6.4}$$

Expression for $\Delta(\phi_1, \phi_2)$ for arbitrary meniscus of nonzero curvature is too long to be presented here.

6.1. Stability of cylinder menisci Cyl

Specify the above formulas for Cyl meniscus,

$$\begin{aligned} &B=0, \quad \bar{r}=1, \quad \bar{z}=\phi, \quad \bar{w}_1=\sin\phi, \quad \bar{w}_2=\cos\phi, \quad \bar{w}_3=1,\\ &L=M=N=0, \quad J_1=-\cos\phi, \quad J_2=\sin\phi, \quad J_3=\phi,\\ &\eta_j=R_j'(\psi_j^*), \quad K_j=\xi_j, \quad S_H=1. \end{aligned} \tag{6.5}$$

Expressions for $\Delta_{Cyl}(\phi_1,\phi_2)$ and matrix elements P_{ij} read

$$\Delta_{Cyl}(\phi_1,\phi_2)=\Delta\phi\,\Gamma_1\left(\frac{\Delta\phi}{2}\right)\sin\Delta\phi, \quad \Gamma_1(x)=1-\frac{\tan x}{x}, \quad \Delta\phi=\phi_1-\phi_2,$$

$$P_{11}=P_{22}=\Delta\phi\,\Gamma_1\,(\Delta\phi)\cos\Delta\phi, \quad P_{12}=-\Delta\phi\Gamma_2(\Delta\phi), \quad \Gamma_2(x)=1-\frac{\sin x}{x}.$$

6.1.1. Cyl meniscus between two plates. We have $\theta_1=\theta_2=\pi/2$ and $R_j=\psi_j$, $Z_j=d$, $K_j=0$, leading to

$$Q_{11}=Q_{22}=\frac{\Gamma_1\,(\Delta\phi)}{\Gamma_1\,(\Delta\phi/2)}\cot\Delta\phi, \quad Q_{12}=-\frac{\Gamma_2\,(\Delta\phi)}{\Gamma_1\,(\Delta\phi/2)}\csc\Delta\phi,$$
$$Q_{33}=-\frac{1}{\Gamma_1\,(\Delta\phi/2)}.$$

There are no conjugate points in region $\Delta_{Cyl}(\phi_1,\phi_2)<0$, i.e., $\Delta\phi<2\pi$. The stability domains $\mathsf{Stab}(\Delta\phi)$ for three different BCs are the following

(a) fixed endpoints: $\Delta_{Cyl}<0 \;\Rightarrow\; 0<\Delta\phi<2\pi$,

(b) one endpoint is free and another is fixed: $Q_{11}>0 \;\Rightarrow 0<\Delta\phi<\varkappa\pi$,

(c) free endpoints: $Q_{33}>0 \;\Rightarrow\; 0<\Delta\phi<\pi$,

where $\varkappa=\min\{x_* \mid \tan x_*=x_*,\ x_*>0\}\simeq 1.4303$. Stability of Cyl meniscus between two plates is well studied and often compared [13,23] to the Plateau–Rayleigh instability of a slow flowing liquid jet of infinite length. Its threshold coincides with the case (a) above in the following sense: The jet of the circular cross section is stable if the length of fluctuations does not exceed the circumference.

6.1.2. Cyl meniscus between two ellipsoids or plate and ellipsoid. Making use of parametrization in Sect. 5.1.2 allows anisotropy ϵ to get both positive and negative values that distinguishes the exterior (convex) ellipsoid shape ($\epsilon>0$) and its interior (concave, or hollow) shape ($\epsilon<0$),

$$\frac{Q_{jj}}{A^2}=\frac{\epsilon_j\sin\psi_j^*\cos\psi_j^*}{\epsilon_j^2\sin^2\psi_j^*+\cos^2\psi_j^*}+\frac{P_{jj}\cos^2\psi_j^*}{\Delta_{Cyl}}, \quad \frac{Q_{12}}{A^2}=\frac{P_{12}\cos\psi_1^*\cos\psi_2^*}{\Delta_{Cyl}},$$

where P_{ij} are given in Sect. 6.1. Consider a case of Cyl between equal ellipsoids.

The stability criteria (4.11) give rise to the SD boundaries by equation,

$$\cot\frac{\Delta\phi}{2}+\frac{\epsilon\tan\psi^*}{\epsilon^2\sin^2\psi^*+\cos^2\psi^*}=0, \tag{6.6}$$

that results in solutions for spheres (see Fig. 6a, for $\epsilon=1$ it coincides with that of reported in [25],

$$\psi^*=\frac{-\pi+\Delta\phi}{2}, \quad 1\le\frac{\Delta\phi}{\pi}\le 2 \quad \text{and} \quad \psi^*=\frac{\pi-\Delta\phi}{2}, \quad 0\le\frac{\Delta\phi}{\pi}\le 1.$$

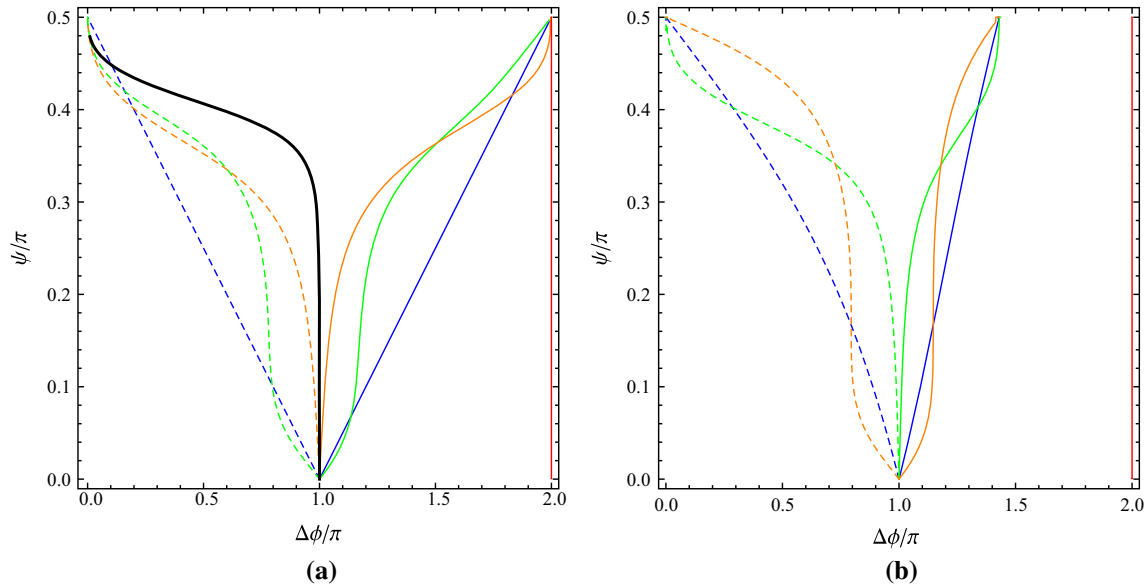

FIG. 6. **a** The right boundaries of SD for Cyl menisci between two solid (*plain*) and hollow (*dashed*) ellipsoids shown in *blue* $\epsilon_j = 1(-1)$, *green* $\epsilon_1 = 3(-3)$, $\epsilon_2 = 0.1(-0.1)$, and *orange* $\epsilon_1 = 0.05(-0.05)$, $\epsilon_2 = 0.15(-0.15)$. The *thick black curve* corresponds to Cyl meniscus between solid and hollow ellipsoids ($\epsilon_1 = -\epsilon_2 = 0.05$). **b** The right boundaries of SD for Cyl menisci between plate and convex (*plain*) or hollow (*dashed*) ellipsoids shown in *blue* $\epsilon_1 = \epsilon_2 = 1(-1)$, *orange* $\epsilon_1 = \epsilon_2 = 3(-3)$, and *green* $\epsilon_1 = \epsilon_2 = 0.1(-0.1)$. The *left boundary* of SD in both (**a**, **b**) coincides with the ψ axis (color figure online)

The case of Cyl meniscus between the plate and ellipsoid gives,

$$\frac{Q_{11}}{A^2} = \frac{\epsilon \sin\psi^* \cos\psi^*}{\epsilon^2 \sin^2\psi^* + \cos^2\psi^*} + \frac{P_{11}\cos^2\psi^*}{\Delta_{Cyl}},$$
$$\frac{Q_{22}}{A^2} = \frac{P_{22}}{\Delta_{Cyl}}, \quad \frac{Q_{12}}{A^2} = \frac{P_{12}\cos\psi^*}{\Delta_{Cyl}}.$$

Its stability is governed by equation,

$$\frac{\tan(\Delta\phi)}{\Gamma_1(\Delta\phi)} - \frac{\epsilon \tan\psi^*}{\epsilon^2 \sin^2\psi^* + \cos^2\psi^*} = 0, \tag{6.7}$$

that results in solutions for sphere ($\epsilon = 1$) upon the plate (see Fig. 6b),

$$\cot\psi^* = \cot\Delta\phi - \frac{1}{\Delta\phi},\ 1 \le \frac{\Delta\phi}{\pi} \le \varkappa, \quad \cot\psi^* = \frac{1}{\Delta\phi} - \cot\Delta\phi,\ 0 \le \frac{\Delta\phi}{\pi} \le 1.$$

6.1.3. Cyl meniscus between two paraboloids or two catenoids. Using parametrization (5.15), write a matrix Q_{ij} and the governing equation for stability of Cyl between two equal paraboloids, $C_i = C$, $a_i = a$, $\nu_i = \nu$ (see Fig. 7a),

$$\frac{Q_{jj}}{A^2} = \rho\frac{\nu-1}{1+\rho^2} + \frac{P_{jj}}{\Delta_{Cyl}}, \quad \frac{Q_{12}}{A^2} = \frac{P_{12}}{\Delta_{Cyl}},$$
$$\rho = \frac{C\nu}{a^{\nu-1}}, \quad \cot\frac{\Delta\phi}{2} + \rho\frac{\nu-1}{1+\rho^2} = 0.$$

The Cyl meniscus between two solid catenoids,

$$R_j = A\psi_j, \quad Z_j = g_j + (-1)^{j+1}AC_j\cosh(b_j\psi_j), \quad C_j, b_j, A > 0, \tag{6.8}$$

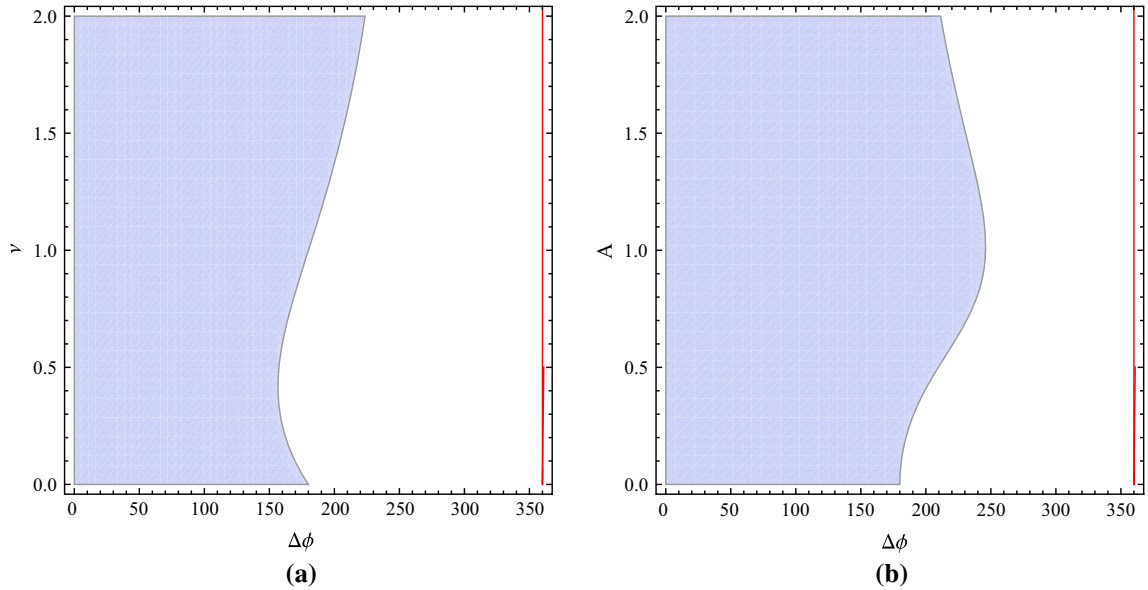

FIG. 7. The SD for Cyl meniscus between **a** two solid paraboloids for $a_i = C_i = 1,\ \nu_1 = \nu_2 = \nu$, and **b** two solid catenoids for $C_i = 1,\ b_1 = b_2 = b$

in the case of equal catenoids, $C_j = C$, $b_j = b$, produces (see Fig. 7b)

$$\frac{Q_{jj}}{A^2} = \frac{Cb^2\cosh b}{1 + C^2b^2\sinh^2 b} + \frac{P_{jj}}{\Delta_{Cyl}},$$
$$\frac{Q_{12}}{A^2} = \frac{P_{12}}{\Delta_{Cyl}}, \quad \cot\frac{\Delta\phi}{2} + \frac{Cb^2\cosh b}{1 + C^2b^2\sinh^2 b} = 0.$$

6.2. Stability of nonzero curvature menisci between two plates

In a variety of axisymmetric menisci with $H \neq 0$ between two solid bodies, we focus on the simple case of two plates and present $\mathsf{Stab}_2(\phi_1, \phi_2)$ for all menisci types. An importance of the two plates setup is based on the statement [7]: *every stable connected configuration is rotationally symmetric*, i.e., axisymmetric LB between two plates under 3D asymmetric perturbations does not bifurcate to any stable 3D asymmetric LB. The stability triangle for Sph menisci in Fig. 8b describes a single Sph segment trapped between two plates. Its right corner $\phi_1 = -\phi_2 = 180^\circ$ corresponds to the whole sphere with contact angles $\theta_1 = \theta_2 = \pi$ embedded between two plates. The SD for Und menisci in Fig. 8c, d are intermediate domains in the range $0 < B < 1$ between Cyl and Sph menisci. The existence of *IP* in the Und meridional profile $\mathcal{M}_U$ is governed by requirement:

$$\phi_2 \le \phi_U^{ip} \le \phi_1, \quad \bar{z}'(\phi_U^{ip})\bar{r}''(\phi_U^{ip}) - \bar{z}''(\phi_U^{ip})\bar{r}'(\phi_U^{ip}) = 0 \ \Rightarrow\ \cos\phi_U^{ip} = -B.$$

A value ϕ_U^{ip} has important property, namely, from (4.12) we obtain

$$Q_{33}(\phi_U^{ip}, -\phi_U^{ip}) = 0. \tag{6.9}$$

In Sect. 6.2.1, we give detailed discussion of ϕ_U^{ip} relationship to Und stability.

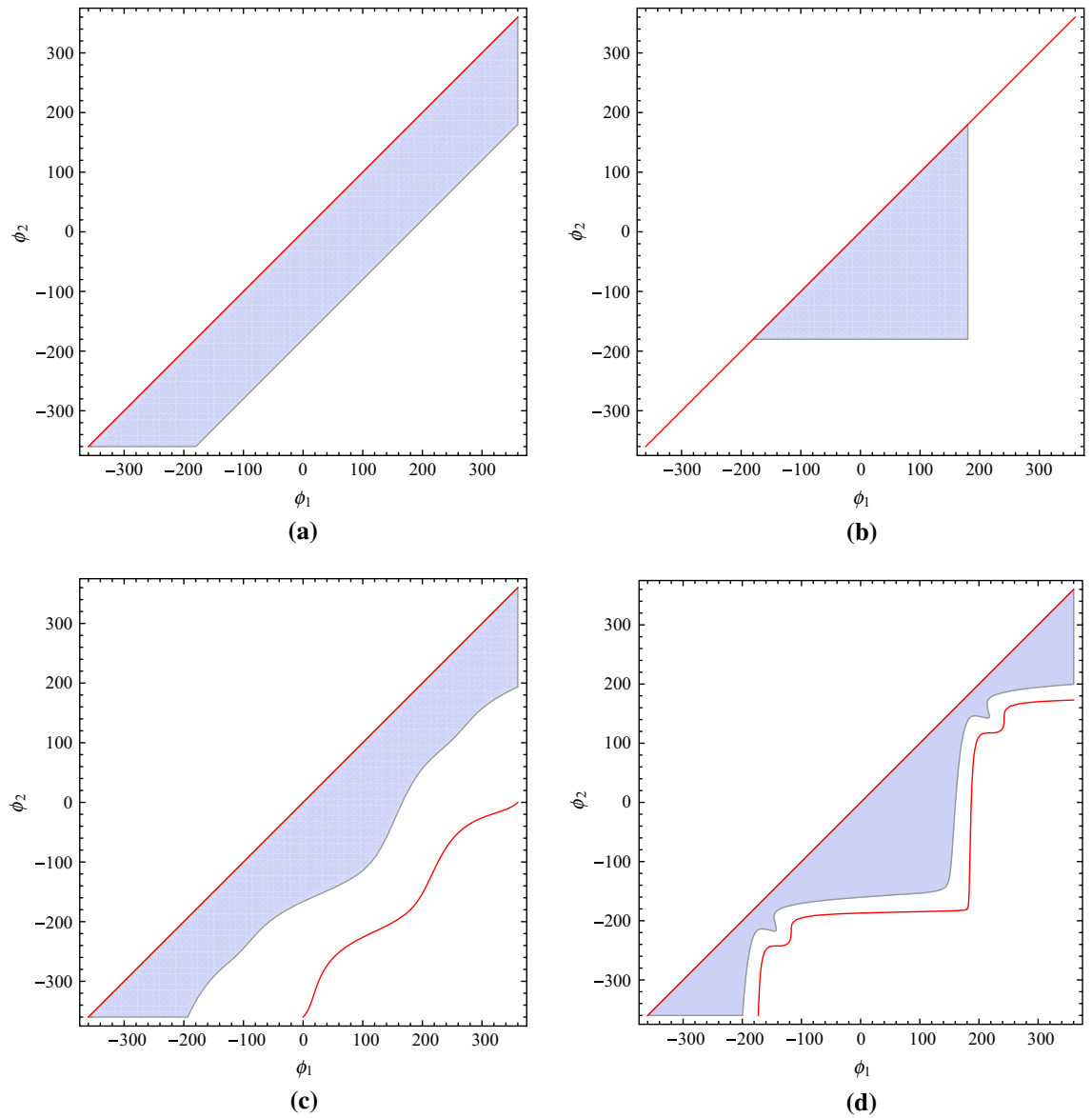

FIG. 8. The SD for **a** Cyl, $B = 0$, **b** Sph, $B = 1$, and two Und menisci, **c** $B = 0.3$ and **d** $B = 0.8$, between two plates. The *red curves* in (**c**, **d**) show the location of conjugate points

The arrangement of the planar solids gives rise to one more symmetry properties of Q_{ij}. Since $Z_j'(\psi_j) = 0$ then according to (5.3, 5.7, 5.8) and (6.2), we have $\bar{z}', \bar{z}_j'', U_j, \eta_j \propto S_H$ and therefore

$$Q_{ij}(S_H) = Q_{ij}(-S_H). \tag{6.10}$$

The SD for Nod menisci in Fig. 9 differ from the rest of diagrams and comprise two different sort of sub-diagrams: Nod menisci with $H > 0$ and $H < 0$. In the case of two solid plates, the positive curvature H corresponds to the convex part of the Nod meridional profile $\mathcal{M}_N$, while the negative H produces its concave segment, which meet at ϕ_N^{ip} such that $z'(\phi_N^{ip}) = 0$, i.e., $\cos\phi_N^{ip} = -B^{-1}$. This justifies the nonexistence of Nod meniscus with both its convex and concave parts.

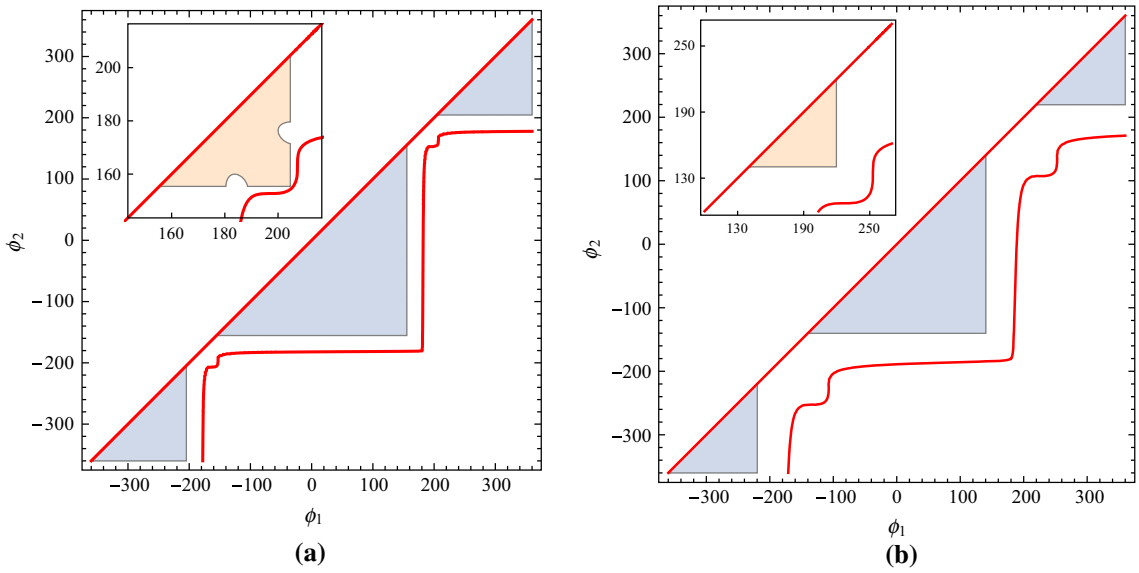

FIG. 9. The SD for Nod menisci between two plates, with **a** $B = 1.1$ and **b** $B = 1.3$. Different types of Nod menisci curvature are shown in *violet-blue* ($H > 0$) and *orange* ($H < 0$) colors. The *orange domain* is accompanied with its twin shifted by 360° in ϕ_1, ϕ_2 (color figure online)

6.2.1. Und menisci with inflection point between two plates. In this section, we verify three statements [1,7,23,24] about stability of Und menisci with free contact points between two plates with contact angles θ_1, θ_2. We also present a new statement summarizing our investigations on stability domain.

1. *If* $\theta_1 = \theta_2 = \pi/2$ *the* Und *menisci are unstable* [1,14,23].

The Und menisci with such BC have necessarily one or more *IPs*: one *IP* for $\phi_1 = n\pi, \phi_2 = (n-1)\pi$, two *IP*s if $\phi_1 = n\pi, \phi_2 = (n-2)\pi$, etc., where n is an integer. However, for $n \geq 2$ a criterion (3.13) is broken, i.e., the conjugate points appear. So there remains one *IP* and a direct calculation of Q_{33} gives for $0 < m < 1$,

$$4\frac{Q_{33}(0,-\pi)}{(1-B)^2} = [3E(m) - K(m)]\,[E(m) - K(m)] + m^2 K(m)\,[2E(m) - K(m)] < 0,$$

where $K(m)$ and $E(m)$ denote the complete elliptic integral of the first and second kind. The last inequality may be verified numerically. In Fig. 10, we present detailed locations of Und menisci with $B = 0.3$ in the sense of its stability w.r.t. the boundaries $\Delta(\phi_1, \phi_2) = 0$ (*the red curve* $\mathfrak{R}$) and $Q_{33}(\phi_1, \phi_2) = 0$ (*the gray curve* $\mathfrak{G}$). The points $C(\phi_1 = 0, \phi_2 = -\pi)$ and $C'(\phi_1 = \pi, \phi_2 = 0)$ lie in unstable zone.

2. *If* $\theta_1 = \theta_2$ *there are no stable menisci with one or more IPs* [7], *Thm 5.7.*

All Und menisci with $\theta_1 = \theta_2$ and without *IP* have the endpoints satisfying $\phi_1 + \phi_2 = 0$. In Fig. 10, they belong to the interval OD of the *blue line* $\mathfrak{B}$ and are stable. There are two different ways to generate *IP*.

First, allow ϕ_1 to grow by preserving the above equality that leaves the meniscus symmetric w.r.t. reflection plane between two plates. When $\phi_1 = \phi_U^{ip}$ there appears a couple of *IPs* (see Fig. 10b), i.e., *IP*s are born on both plates simultaneously. We cannot make any conclusion about stability of this meniscus in the framework of Weierstrass' theory. But all menisci with $\phi_1 + \phi_2 = 0$, $\phi_1 > \phi_U^{ip}$, having two *IPs*, are unstable. In Fig. 10, they belong to $\mathfrak{S}$ beyond the point D. Thus, the range of equal contact angles θ for stable menisci without *IP* reads $\pi/2 < \theta < \phi_U^{ip}$ for convex Und and $\pi - \phi_U^{ip} < \theta < \pi/2$ for concave Und.

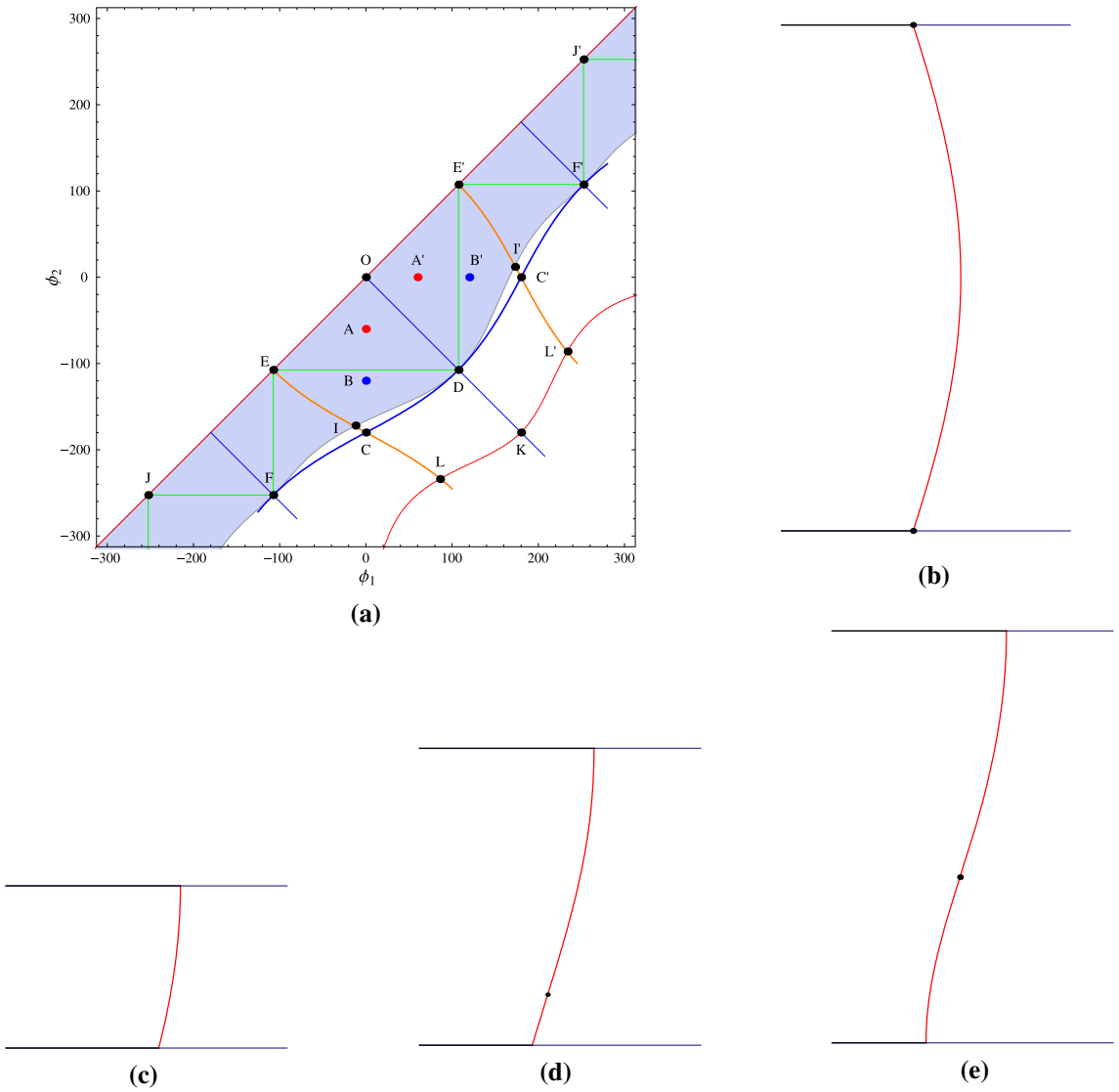

FIG. 10. The SD for Und menisci with $B = 0.3$. **a** The *green lines* $\mathfrak{Z}$ show *IP* separation from a plate. The *dots mark* menisci shown in: **b** point **D** for $\phi_1 = -\phi_2 = \phi_U^{ip} = 107.46°$ (two *IPs* at the plates) **c** point **A** for $\phi_1 = 0°, \phi_2 = -60°$ (stable meniscus without *IP*), **d** point **B** for $\phi_1 = 0°, \phi_2 = -120°$ (stable meniscus with one *IP*), **e** point **C** for $\phi_1 = 0°, \phi_2 = -180°$ (unstable meniscus with one *IP*) (color figure online)

Another way to generate *IP* with $\theta_1 = \theta_2$ is to break the reflection symmetry $\phi_1 + \phi_2 \neq 0$, where $\phi_1 < \phi_U^{ip}$ and $\phi_2 < -\phi_U^{ip}$. Making use of (6.2) for $\tan\theta_j = (-1)^j z'(\phi_j)/r'(\phi_j)$ write an equality for ϕ_1, ϕ_2,

$$P(\phi_1) + P(\phi_2) = 0 \quad \Rightarrow \quad \tan\frac{\phi_1}{2}\tan\frac{\phi_2}{2} = -\frac{1+B}{1-B}, \tag{6.11}$$

where $P(\phi) = (1 + B\cos\phi)/(B\sin\phi)$. Calculation of Q_{33} in accordance with (4.11) and (6.11) leads to cumbersome expression. Instead of its analysis, we present in Fig. 10 the *blue curve* $\mathfrak{B}$ given by equation (6.11) and observe that $\mathfrak{B}$ always lies in instability zone, confirmed by numerical calculation of Q_{33} for $0 < B < 1$. The curves $\mathfrak{B}$ and $\mathfrak{G}$ are tangent at points F, D, H.

There is one more important conclusion: Und meniscus with reflection symmetry ($\theta_1 = \theta_2$) and fixed CL at two plates are stable even when two *IPs* exist. This follows from an observation that an interval DK at Fig. 10 is above the curve $\mathfrak{R}$. The point $K(\phi_1 = \pi, \phi_2 = -\pi)$ marks unstable Und meniscus of entire period with four *IPs* when two of them are separated from the plates.

3. *If* $\theta_1, \theta_2 \neq \pi/2$, $\theta_1 + \theta_2 = \pi$ *there are stable menisci of large volume that have IPs* [24], *Remark 3.2.*

Making use of (6.2) and identity $\tan(\theta_1 + \theta_2) = 0$ write a relation for the angles ϕ_1, ϕ_2 valid for the arbitrary volume's value,

$$P(\phi_1) - P(\phi_2) = 0 \quad \Rightarrow \quad \tan\frac{\phi_1}{2}\tan\frac{\phi_2}{2} = \frac{1+B}{1-B}. \tag{6.12}$$

Similar to the previous case considered in Fig. 10, the *brown curves* given by Eq. (6.12) and observe that they always pass through the point C and cross transversely the curve $\mathfrak{G}$ at point I which separates the menisci in two families: stable with one *IP* (at interval GI) and unstable (beyond the point I). Note that the stable menisci without *IP* are forbidden. Regarding the claim *'stable menisci of large volume that have IPs'*, we have found it incorrect. Indeed, the whole segment E'I belongs to the stability region and it remains true when we approach the point E', i.e., when $\phi_2 \to \phi_1$ that manifests volume decrease up to an arbitrary small value. Therefore, we make a statement slightly different: *if* $\theta_1 + \theta_2 = \pi$, *then only menisci with a single IP are stable.*

Summarize the above results: The stability region $\mathsf{Stab}_2(\phi_1, \phi_2)$ of Und meniscus between two plates with free CL is represented in Fig. 10 by interior of domain decomposed in subdomains

$$\mathsf{Stab}_2(\phi_1,\phi_2) = \{DIFE\}_1 \cup \{DI'F'E'\}_1 \cup \{JEF\}_0 \cup \{EOE'DE\}_0 \cup \{J'E'F'\}_0$$

where a subscript stands for a number of *IP* in stable meniscus.

4. Finish this section with two other setups for Und menisci between two plates: $\theta_1 \pm \theta_2 = \pi/2$, which differ from those discussed in [1,7,23,24]. Using formulas (6.2), write an equality which is not solvable in ϕ_1, ϕ_2 for all B,

$$P(\phi_1)P(\phi_2) = \mp 1, \ |P(\phi)| \geq \left|P\left(\phi_U^{ip}\right)\right| = \frac{\sqrt{1-B^2}}{B} \ \Rightarrow \ \exists \ \phi_j \in \Re \quad \text{if } B \geq \frac{1}{\sqrt{2}}.$$

The upper (lower) sign in last equality corresponds to upper (lower) sign in $\theta_1 \pm \theta_2$. For $B = 1/\sqrt{2}$ there exist two pointwise solutions of equation $P(\phi_1)P(\phi_2) = \mp 1$,

$$\text{a):} \quad \frac{\phi_1}{5} = \frac{\phi_2}{3} = \frac{\pi}{4} \quad \text{and} \quad \frac{\phi_1}{5} = \frac{\phi_2}{3} = -\frac{\pi}{4}$$
$$\text{b):} \quad \frac{\phi_1}{5} = \frac{\phi_2}{5} = \pm\frac{\pi}{4} \quad \text{and} \quad \frac{\phi_1}{3} = \frac{\phi_2}{3} = \pm\frac{\pi}{4}.$$

However, when $B > 1/\sqrt{2}$ the solutions are represented by curves L_a and L_b in the halfplane $\{\phi_2 < \phi_1\}$: L_a passes through unstable and stable (without *IP*) zones, while L_b exists only in stable zones with and without *IP* (see Fig. 11).

7. Conclusion

We derive the stability criterion in the isoperimetric problem with free endpoints and apply it to theory of axisymmetric LB between two axisymmetric solid bodies without gravity to determine the stability of menisci with free CL. The former presents a new result which has not appeared earlier in classical calculus of variations, while the latter allows to obtain an explicit expression for stability criterion which was not widely discussed in the literature for arbitrary shapes of solid body and liquid bridge.

Our non-spectral theory of stability of axisymmetric LB upon axisymmetric LB perturbations may be extended to any asymmetric LB perturbations. For this purpose, one can use Lemma 2.1 in [23]

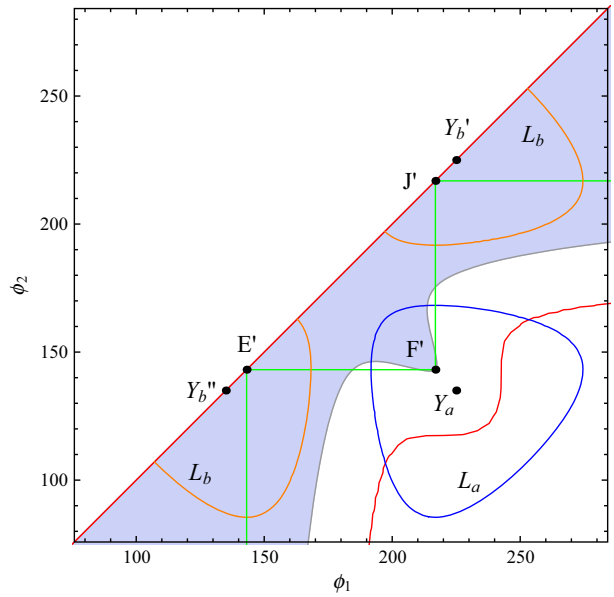

FIG. 11. The SD for Und menisci with $B = 0.8$ (a part of Fig. 8d). The *green* line shows the position of *IPs*. The dots mark menisci contacting the lower and upper plates at ϕ_2 and ϕ_1, respectively: (Y_a) $\phi_1 = 225°, \phi_2 = 135°$, (Y_b') $\phi_1 = \phi_2 = 225°$, (Y_b'') $\phi_1 = \phi_2 = 135°$, in accordance with Sect. 6.2.1. *Curves* L_a and L_b describe Und menisci satisfying $\theta_1 + \theta_2 = \pi/2$ and $\theta_1 - \theta_2 = \pi/2$, respectively

on elimination of the asymmetric perturbations in stability problem of axisymmetric LB. This strong statement is based on the Schwarz symmetrization in functional analysis and belongs to a wide class of isoperimetric inequalities. It supports also a coincidence of stability domains Stab_2 calculated in spectral and non-spectral theories in all setups considered earlier: Cyl between two plates [1,23] in Sect. 6.1.1, Cyl between two equal convex spheres [25] in Sect. 6.1.2, Und between two plates with specific contact angles, $\theta_1 = \theta_2$ [7] and $\theta_1 + \theta_2 = \pi$, $\theta_1, \theta_2 \neq \pi/2$, [24] in Sect. 6.2.1, Cat between two plates [29] in Sect. 5.1.1.

In addition to usually treated menisci between two planar or two spherical solids, we consider a wide range of axisymmetric solid shapes: Cyl menisci between two paraboloids, catenoids, convex and hollow ellipsoids and Cat between plate and sphere. In fact, this list may be continued without limitation.

Beyond the scope of the present paper, there are left much more difficult cases of Und, Nod and Sph menisci stability between non-planar solids: Here a new effect of LB existence begin to interfere with the stability of LB. We plan to classify different types of LB nonexistence and study their influence on stability domains in the separate paper.

Acknowledgements

The useful discussions with O. Lavrenteva are appreciated. The research was supported in part (LGF) by the Kamea Fellowship.

References

1. Athanassenas, M.: A variational problem for constant mean curvature surfaces with free boundary. J. für Math. **377**, 97–107 (1987)
2. Beer, A: Tractatus de Theoria Mathematica Phenomenorum in Liquidis Actioni Gravitatis Detractis Observatorum. George Carol, Bonn (1857)

3. Bolza, O: Lectures on the Calculus of Variations. University of Chicago Press, Chicago (1904)
4. Courant, R., Hilbert, D.: Methods of Mathematical Physics. Vol. 1, Wiley, New York (1989)
5. Delaunay, C.E.: Sur la surface de révolution dont la courbure moyenne est constante. J. Math. Pure Et App. **16**, 309–315 (1841)
6. Erle, M.A., Gillette, R.D., Dyson, D.C.: Stability of interfaces of revolution—the case of catenoid. Chem. Eng. J. **1**, 97–109 (1970)
7. Finn, R., Vogel, T.: On the volume infimum for liquid bridges. Z. Anal. Anwend. **11**, 3–23 (1992)
8. Gelfand, I.M., Fomin, S.M.: Calculus of Variations. Dover, Mineola (2000)
9. Gillette, R.D., Dyson, D.C.: Stability of fluid interfaces of revolution between equal solid plates. Chem. Eng. J. **2**, 44–54 (1971)
10. Hadzhilazova, M., Mladenov, I., Oprea, J.: Unduloids and their geometry. Arch. Math. **43**, 417–429 (2007)
11. Howe, W.: Die Rotations-Flächen welche bei vorgeschriebener Flächengrösse ein möglichst grosses oder kleines Volumen enthalten. Inaug.-Dissert. Friedrich-Wilhelms-Universität zu Berlin (1887)
12. Kenmotsu, K.: Surfaces of revolution with prescribed mean curvature. Tohoku Math. J. **32**, 147–153 (1980)
13. Langbein, D.: Capillary Surfaces: Shape–Stability–Dynamics, in Particular Under Weightlessness. Springer Tracts in Modern Physics, Vol. 178. Springer, New York (2002)
14. Lubarda, V.A.: On the stability of a cylindrical liquid bridge. Acta Mech. **226**, 233–247 (2015)
15. Myshkis, A.D., Babskii, V.G., Kopachevskii, N.D., Slobozhanin, L.A., Tyuptsov, A.D.: Lowgravity Fluid Mechanics. Springer, New York (1987)
16. Orr, F.M., Scriven, L.E., Rivas, A.P.: Pendular rings between solids: meniscus properties and capillary forces. J. Fluid Mech. **67**, 723–744 (1975)
17. Plateau, J.A.F.: Statique expérimentale et théoretique des liquides. Gauthier-Villars, Paris (1873)
18. Roy, R.V., Schwartz, L.W.: On the stability of liquid ridges. J. Fluid Mech. **391**, 293–318 (1999)
19. Rubinstein, B.Y., Fel, L.G.: Theory of axisymmetric pendular rings. J. Colloid Interface Sci. **417**, 37–50 (2014)
20. Slobozhanin, L.A., Alexander, J.I.D., Fedoseyev, A.I.: Shape and stability of doubly connected axisymmetric free surfaces in a cylindrical container. Phys. Fluids **11**, 3668–3677 (1999)
21. Strube, D.: Stability of spherical and catenoidal liquid bridge between two parallel plates in absence of gravity. Microgravity Sci. Technol. **4**, 263–269 (1991)
22. Sturm, M.: Note, Á l'occasion de l'article précédent. J. Math. Pure Et App. **16**, 315–321 (1841)
23. Vogel, T.: Stability of a liquid drop trapped between two parallel planes. SIAM J. Appl. Math. **47**, 516–525 (1987)
24. Vogel, T.: Stability of a liquid drop trapped between two parallel planes, II: general contact angles. SIAM J. Appl. Math. **49**, 1009–1028 (1989)
25. Vogel, T.: Non-linear stability of a certain capillary problem. Dyn. Contin. Discrete Impuls. Syst. **5**, 1–16 (1999)
26. Vogel, T.: Convex, rotationally symmetric liquid bridges between spheres. Pacific J. Math. **224**, 367–377 (2006)
27. Weierstrass, K.: Mathematische Werke von Karl Weierstrass, 7, Vorlesungenüber Variationsrechnung, Leipzig, Akademische Verlagsgesellschaft (1927)
28. Wente, H.C.: The symmetry of sessile and pendant drops. Pacific J. Math. **88**, 387–397 (1980)
29. Zhou, L.: On stability of a catenoidal liquid bridge. Pacific J. Math. **178**, 185–198 (1997)

Leonid G. Fel
Department of Civil Engineering
Technion – Israel Institute of Technology
32000 Haifa
Israel
e-mail: lfel@technion.ac.il

Boris Y. Rubinstein
Stowers Institute for Medical Research
1000 E 50th St
Kansas City
MO 64110
USA
e-mail: bru@stowers.org

(Received: April 30, 2015; revised: June 22, 2015)